Impurity and spin-fluctuation effects in antiferromagnetic superconductors*

M. J. Nass† and K. Levin
The James Franck Institute and the Department of Physics, The University of Chicago, Chicago, Illinois 60637

G. S. Grest‡
The Department of Physics, Purdue University, West Lafayette, Indiana 47907

(Received 6 November 1981)

We derive the superconducting density of states $N_s(\omega)$ of an antiferromagnetic superconductor in the presence of impurities and spin fluctuations. We use a self-consistent ansatz for the Green's function G and our previous mean-field-theory results. $N_s(\omega)$ depends on four functions of frequency: the renormalized frequency $\tilde{\omega}$, gap $\tilde{\Delta}$, molecular field $\tilde{H}_Q$, and "pseudogap" $\tilde{\Omega}$. Equations for these four parameters are set up in general and solved for the case of elastically scattering impurities and spin fluctuations. In the absence of any disorder the density of states has structure at the gap frequency Δ and at $\omega = |\Delta \pm H_Q|$, where H_Q is the (screened) molecular field. Most of our numerical work for dirty superconductors is based on a "quasi-three-dimensional" approximation which appears to be reasonable, although it underestimates gaplessness and overestimates the strength of the subsidiary peaks at $|\Delta \pm H_Q|$. We find in this approximation that magnetic impurities behave as might be expected but that nonmagnetic impurities can make an antiferromagnetic (AF) superconductor gapless at moderate concentrations. As the concentration is increased still further, the nonmagnetic impurities "screen" out the molecular field, a gap reopens, and $N_s(\omega)$ obtains its BCS value. In the process of solving for $N_s(\omega)$, we have simultaneously solved the self-consistent equations for Δ (as well as H_Q) as a function of temperature T for dirty superconductors. We find that both Δ and the thermodynamic critical field H_c exhibit structure at the magnetic ordering temperature T_M. As in the case of our previous mean-field-theory results, the behavior of H_c is similar to that of H_{c2}, observed in the ternary compounds. When spin-fluctuation effects are included, $N_s(\omega)$ and its derivative are found to exhibit structure at the spin-wave frequencies. In analogy with phonons in strong-coupling superconductors, this observation suggests that a measurement of $N_s(\omega)$ in AF superconductors can provide detailed information about the dynamic structure factor for the localized spins.

I. INTRODUCTION

Considerable attention[1] has recently been focused on the ternary rare-earth (R) compounds of the type $R\mathrm{Mo}_6\mathrm{S}_8$ and $R\mathrm{Rh}_4\mathrm{B}_4$ because many of these exhibit both magnetic and superconducting order. Of this class of compounds, only those which undergo antiferromagnetic (AF) order, arising from R spins, have thus far been unambiguously shown to have spatially coexistent magnetic and superconducting order. It might seem reasonable that AF order will not destroy superconductivity since it is not associated with macroscopic magnetic molecular fields and since, presumably, only small regions of the Fermi surface are profoundly affected by these fields. However, spin fluctuations about the magnetically ordered state will scatter the Cooper pairs and weaken superconductivity. It is, thus, not *a priori* clear under what circumstances superconductivity and AF order are compatible.

To date, theories of the AF superconductors have not simultaneously included these important spin-fluctuation effects and the effects of the mag-

netic molecular fields. It is the purpose of the present paper to build on our previous Letter[2] (called paper L1), which primarily treated the AF order at the level of mean-field theory, and to include spin-fluctuation effects. Furthermore, because the formalism for treating impurity scattering is closely analogous to that which includes spin fluctuations and because the ternary R compounds are not highly pure, we will discuss at some length impurity scattering. Associated with "dirt effects" are several very interesting phenomena.[2]

Our ultimate aim in this work is to obtain from the "renormalized" Green's function G, the superconducting density of states $N_s(\omega)$. It is this quantity which can be directly measured in (future) tunneling experiments and which contains the most detailed information about the delicate interplay of superconductivity and magnetism. In the process of calculating G and $N_s(\omega)$ we also obtain (i) the temperature dependence of the order parameter Δ and thermodynamic critical field H_c, and (ii) the frequency dependence of the renormalized gap parameter $\tilde{\Delta}(\omega)$, magnetic molecular field $\tilde{H}_Q(\omega)$, and renormalized frequency $\tilde{\omega}(\omega)$. Our calculation of G provides a basis for future work dealing with *external* perturbations in the AF superconductors, as, for example, electromagnetic fields.

The first workers to study theoretically AF superconductors considered[3] the effects of spin fluctuations in the paramagnetic phase. Subsequently, it was proposed[4] that a "new" superconducting pairing (involving magnetic quasiparticle states) was important, but this calculation was later shown[2] to be inapplicable. One-dimensional (1D) systems with no spin or impurity disorder were examined[5] using the usual BCS pairing in the presence of static, uniform magnetic fields. To date, the most detailed study of spin-fluctuation effects in AF superconductors is that of Ramakrishnan and Varma,[6] who discussed pairbreaking effects but ignored the AF molecular field (which we show to be important here). Recent work by Zwicknagl and Fulde[7] is based on the "new" pairing state and its effects on the electron-phonon interaction. They studied H_{c2} in AF superconductors; their work did not include (inelastic) spin-fluctuation effects.

The present work is unique in that it includes both spin-fluctuation and disorder effects while simultaneously treating the AF molecular field, H_Q. Our focus is on $N_s(\omega)$, although we also calculate the thermodynamic critical field $H_c(T)$ [from whch H_{c2} may be obtained using the phenomenological relation $H_{c2}=H_c\sqrt{2}\kappa(T)$]. Because we include H_Q in our strong-coupling formalism, we obtain four (rather than two) coupled Eliashberg-type equations for the renormalized gap $\tilde{\Delta}$, frequency ω, molecular field $\tilde{H}_Q$, and "pseudogap" $\tilde{\Omega}$ (which will be defined below). These are exactly solved numerically when elastically scattering impurities and spin fluctuations are present.

In Sec. II we review and extend our previous mean-field results and present an ansatz for the renormalized Green's function G. This ansatz leads to four equations for the unknowns $\tilde{\Delta}$, $\tilde{\omega}$, $\tilde{H}_Q$, and $\tilde{\Omega}$ which must be solved self-consistently with the (weak-coupling) equations for Δ and H_Q. While we set up the formalism quite generally, we discuss in detail the "quasi-three-dimensional (3D) approximation", which is more amenable to numerical solutions. In Sec. III, we study the effects of nonmagnetic impurities in 1D AF superconductors. This section lays the groundwork for our quasi-3D studies of Sec. IV. It is illuminating because it highlights the similarity in the formalism for treating nonmagnetic impurities in AF superconductors with that for treating magnetic impurities in the usual superconductors.[8,9]

Section IV A presents a detailed comparison between the quasi-3D approximation and a more exact 3D treatment which we discussed in paper L1. We are able to do this quantitatively only for pure superconductors. However, our results suggest that the quasi-3D approximation is reasonably good when the superconductor is dirty. Generally, the quasi-3D approximation underestimates gaplessness and overestimates the importance of subsidiary peaks in $N_s(\omega)$ which appear away from the gap frequency.

In Sec. IV B we study the effects of magnetic and nonmagnetic impurities on $N_s(\omega)$ in the quasi-3D approximation. Our results are presented for a range of lifetime parameters τ_1 and τ_2. Section IV C deals with finite-temperature properties of the superconductor. Following the formalism of Skalski *et al.*,[10] we compute Δ and H_c^2 as a function of temperature T. Both Δ and H_c^2 show sharp structure at the magnetic-ordering temperature T_M, similar to that found in the mean-field theory of paper L1.

In Sec. V we set up the equations for $\tilde{\omega}$, $\tilde{\Delta}$, $\tilde{H}_Q$, and $\tilde{\Omega}$ when both spin fluctuations and impurities are present. We numerically solve them using a simple model for the dynamic susceptibility. Sharp structure in $N_s(\omega)$ appears at the spin-wave frequency ω_s. Away from ω_s, the density of states

does not change appreciably from the case where spin fluctuations are absent. Finally in Sec. VI we list our conclusions.

II. GENERAL THEORY

In this section we present the general theory of fluctuation effects and impurity scattering in AF superconductors. We assume that, as in the Chevrel and rhodium-boride compounds, the system contains two[11] types of electrons. The first, the f electrons on the rare-earth atoms, have localized moments which undergo AF order. The second, the d conduction electrons, form superconducting pairs. Our Hamiltonian is thus

$$\mathcal{H}=\mathcal{H}^0+\mathcal{H}^{ee}+\mathcal{H}^{ex} , \tag{2.1}$$

where

$$\mathcal{H}^0=\sum_{k,\sigma}\epsilon_k C^\dagger_{k\sigma}C_{k\sigma} , \tag{2.2}$$

$$\mathcal{H}^{ee}=\sum_{\substack{kk'\sigma\sigma'\\ q}} V_{kk'q}C^\dagger_{k+q\sigma} \times C^\dagger_{k'-q\sigma'}C^\dagger_{k'\sigma'}C_{k\sigma} , \tag{2.3}$$

and

$$\mathcal{H}^{ex}=-\tfrac{1}{2}\sum_{kk'j\sigma\sigma'} J(k-k')\exp[i(\vec{k}-\vec{k}')\cdot\vec{R}_j] \times\vec{S}_j\cdot\vec{s}\,C^\dagger_{k\sigma}C_{k'\sigma'} . \tag{2.4}$$

Here $\mathcal{H}^0$ is the kinetic-energy term for the d electrons. $\mathcal{H}^{ee}$ describes the attractive phonon-mediated electron-electron interaction which leads to Cooper pairing. $\mathcal{H}^{ex}$ describes the conduction-electron-f-electron spin-spin exchange.[11] Here, $\vec{S}_j$ is the spin operator for the f electron at site R_j; $\vec{s}$ is the conduction-electron spin operator and $J(\vec{k}-\vec{k}')$ is the exchange interaction. In all that follows, we assume J is independent of $(\vec{k}-\vec{k}')$ for simplicity.

We proceed by rewriting $\mathcal{H}^{ex}$ as

$$\mathcal{H}^{ex}=\langle\mathcal{H}^{ex}\rangle+(\mathcal{H}^{ex}-\langle\mathcal{H}^{ex}\rangle) \equiv\langle\mathcal{H}^{ex}\rangle+\mathcal{H}^{fluc} . \tag{2.5}$$

Here $\langle\mathcal{H}^{ex}\rangle$ describes the mean-field approximation to $\mathcal{H}^{ex}$

$$\langle\mathcal{H}^{ex}\rangle=-\sum_{k\sigma}H^0_Q\sigma(C^\dagger_{k\sigma}C_{k+Q\sigma}+C^\dagger_{k+Q\sigma}C_{k\sigma}) , \tag{2.6}$$

and

$$H^0_Q=J\langle S_Q\rangle/2N . \tag{2.7}$$

Here $\langle S_Q\rangle$ is the thermal average of the Fourier transform of S_j which is assumed nonzero in the magnetically ordered state. Throughout this work we will treat H^0_Q as a phenomenological, temperature-dependent quantity. Experiments suggest[12] that at low T, H^0_Q is of the order of 100 K. In principle H^0_Q should be calculated self-consistently, by introducing the rare-earth ion-ion interactions. Furthermore, it is presumably sensitive to impurity effects. At this stage we proceed phenomenologically and ignore these.

In the most general case, superconducting pairing with pair momentum $q=0$ and $q=\pm Q$ should be included in our theory. Ignoring fluctuation effects ($\mathcal{H}^{fluc}=0$) and performing the BCS factorization of Eq. (2.8) amounts to treating the AF superconductor at the level of a "coupled mean-field theory": mean-field theory for both the superconducting and AF order. We explored this theory in detail in paper L1. The full mean-field Hamiltonian we studied there was

$$\mathcal{H}^{mf}=\sum_{k\sigma}\epsilon_k C^\dagger_{k\sigma}C_{k\sigma}-\sum_{k\sigma}H_Q\sigma(C^\dagger_{k\sigma}C_{k+Q\sigma}+C^\dagger_{k+Q\sigma}C_{k\sigma}) \times\left[-\sum_k\Delta C^\dagger_{k\uparrow}C^\dagger_{-k\downarrow}-\sum_k{}'(\Delta_Q C^\dagger_{k+Q\uparrow}C^\dagger_{-k\downarrow}-\Delta_{-Q}C^\dagger_{k\uparrow}C^\dagger_{-k-Q\downarrow})+\text{c.c.}\right] , \tag{2.8}$$

where

$$\Delta=\sum_{k'}V\langle C_{k'}C_{k'}\rangle , \tag{2.9a}$$

$$\Delta_Q=2\sum_{k'}{}'V\langle C_{k'}C_{-k'+Q}\rangle , \tag{2.9b}$$

$$\Delta_{-Q}=2\sum_{k'}{}'V\langle C_{-k'-Q\downarrow}C_{k'\uparrow}\rangle . \tag{2.9c}$$

Here, V is the usual BCS potential which is cut off at ω_c. Throughout this paper we will treat phonon effects in weak-coupling theory although the

strong-coupling generalization is straightforward. The prime in Eqs. (2.8) and (2.9) indicates the sum is only over region I, defined below. We note that H_Q differs from H_Q^0 [defined in Eq. (2.8)] due to screening effects:

$$H_Q = H_Q^0 - \tfrac{1}{2}{\sum_{k'\sigma}}' V\sigma \langle C_{k'\sigma}^\dagger C_{k'+Q\sigma}\rangle \ . \tag{2.10}$$

Formally this result follows from a factorization of Eq. (2.3) in addition to the usual BCS factorization which leads to Eq. (2.9). At temperatures that are low compared to the magnetic transition temperature T_M, $|H_Q - H_Q^0|$ is typically of order Δ and since, away from T_M, $\Delta << H_Q^0$, the screening will have little effect. Near T_M, however, screening effects are more pronounced.

It is convenient to divide the Fermi surface (FS) into two regions called I and II. In region I, both ϵ_k and ϵ_{k+Q} (for $k<0$) are within the BCS cutoff ω_c of the Fermi energy E_F. We treat H_Q exactly only in region I since its effects are most significant there. In region II, which is the remainder of the FS we ignore H_Q, since

$$|H_Q/(\epsilon_k - \epsilon_{k+Q})| << 1 \ ,$$

and therefore it leads to only weak perturbative corrections. With this approximation we may then write down a simple 4×4 matrix representation of $\mathscr{H}^{\rm mf}$ in region I; only the operators $C_{k\uparrow}$, $C_{k+Q\uparrow}$, $C_{-k\downarrow}^\dagger$, and $C_{-k-Q\downarrow}^\dagger$ are coupled. The Hamiltonian may be diagonalized and Δ, Δ_Q, etc., are solved for self-consistently. This procedure was described in detail in paper L1. Implicit in all of this is the reasonable[13] assumption that $H_Q << E_F$ and that the magnetic reciprocal-lattice vector intersects the Fermi surface (in the real ternary compounds), so that the density of states near E_F is modified by the magnetic Brillouin-zone boundary. In paper L1, we pointed out that the fraction of superconducting electrons in region I is related to $\omega_c/k_F Q$. (Throughout this work we use the units $\hbar = 2m = 1$). It is believed that this ratio is of the order of 10–20%.[14]

In 1D systems we noted in L1 that $\Delta_Q = \Delta_{-Q} = 0$ is the only allowed solution of the coupled gap equations. Physically this corresponds to that fact that Q is large compared to the inverse coherence length so that only the usual ($q=0$) pairing corresponds to a free-energy extremum. Using our Green's-function formalism we have derived the coupled gap equations for Δ_Q, Δ_{-Q}, and Δ for 3D systems. These are presented in the Appendix. A numerical solution of these coupled equations yields that $\Delta_Q = -\Delta_{-Q}$ and that $|\Delta_{\pm Q}|$ is one to two percent of Δ for region I containing 10% to 20% of the entire Fermi surface, respectively (with $H_Q = 0.1-0.3\omega_c$). This ratio decreases as H_Q varies outside this range. Because our numerical results yielded a small value for $|\Delta_{\pm Q}|$ and because in what follows we will primarily use the "quasi-3D approximation" (in which $\Delta_{\pm Q}$ is strictly zero), we will henceforth consider $\Delta_{\pm Q}$ to be negligible. That our detailed numerical calculation led to an extremely small value of $|\Delta_{\pm Q}|$ is further evidence against the existence of the so called "new pairing" state.[4,7]

To go beyond our simple mean-field theory we will adopt a generalization of the matrix Green's-function approach, used[5] to treat dilute magnetic impurities in superconductors. To include spin-flip scattering effects (which arise from spin-fluctuation and magnetic impurity scattering) we must represent our Green's function G in the *eight*-dimensional basis

$$\psi^\dagger = (C_{k\uparrow}^\dagger \ \ C_{-k\downarrow}^\dagger \ \ C_{k\uparrow} \ \ C_{-k\downarrow} \ \ C_{k+Q\uparrow}^\dagger \ \ C_{-k-Q\downarrow}^\dagger \ \ C_{k+Q\uparrow} \ \ C_{-k-Q\downarrow}) \ . \tag{2.11}$$

We may write the unperturbed Green's function, corresponding to our coupled-mean-field theory as

$$G_0^{-1}(k,i\omega_n) = i\omega_n - \mathscr{H}^{\rm mf} = i\omega_n - \epsilon_s\rho_3 - \epsilon_a\tau_3\rho_3 - \Delta\rho_2\sigma_2 + H_Q\tau_1\rho_3\sigma_3 \ , \tag{2.12}$$

where $\epsilon_s = \frac{1}{2}(\epsilon_k + \epsilon_{k+Q})$ and $\epsilon_a = \frac{1}{2}(\epsilon_k - \epsilon_{k+Q})$; ω_n is a Matsubara frequency and τ_i, ρ_i, and σ_i are the Pauli matrices on eight-, four-, and two-dimensional vector spaces, respectively. Thus, for example,

$$\tau_1\rho_3\sigma_2 = \begin{bmatrix} 0 & 0 & \sigma_2 & 0 \\ 0 & 0 & 0 & -\sigma_2 \\ \sigma_2 & 0 & 0 & 0 \\ 0 & -\sigma_2 & 0 & 0 \end{bmatrix} ,$$

where each entry is the 2×2 Pauli matrix σ_2.

The renormalized Green's function which includes spin-fluctuation and impurity effects is obtained diagrammatically using the self-consistent Hartree-Fock approximation. We make the ansatz

$$G^{-1}(k,i\omega_n)=i\tilde{\omega}_n-\epsilon_s\rho_3-\epsilon_a\tau_3\rho_3 -\tilde{\Delta}_n\rho_2\sigma_2+\tilde{H}_{Qn}\tau_1\rho_3\sigma_3 +i\tilde{\Omega}_n\tau_1\rho_1\sigma_1 . \quad (2.13)$$

Here, $\tilde{\omega}_n$, $\tilde{\Delta}_n$, $\tilde{H}_{Qn}$, and $\tilde{\Omega}_n$ are unknown functions of ω_n, which are to be determined self-consistently. Note that a new matrix element involving the "pseudogap" $\tilde{\Omega}_n$ is required for self-consistency even though its analog was not present[15] in the bare Green's function G_0. This is similar to what was found previously[8] when considering the effects of Pauli paramagnetism in superconductors.

The interaction of the superconducting electrons with spin fluctuations and/or impurities leads to a self-energy,

$$\Sigma(k,i\omega_n)=G_0^{-1}(k,i\omega_n)-G^{-1}(k,i\omega_n) . \quad (2.14)$$

In the Born approximation, we find for impurity scattering

$$\Sigma(k,i\omega_n)=T\sum_m\int\frac{d^3k'}{(2\pi)^3}\delta(\omega_n-\omega_m) \times U(\vec{k}-\vec{k}')G(k',i\omega_m) \times U(\vec{k}-\vec{k}') , \quad (2.15)$$

where U is the 8×8 matrix scattering potential,[8]

$$U(\vec{k})=U_1(\vec{k})\rho_3+U_2(\vec{k})\vec{S}\cdot\vec{\alpha} . \quad (2.16)$$

Here U_1 and U_2 are the potential and magnetic scattering interactions, respectively, and

$$\vec{\alpha}=\tfrac{1}{2}(1+\rho_3)\vec{\sigma}+\tfrac{1}{2}(1-\rho_3)\sigma_2\vec{\sigma}\sigma_2 .$$

By inserting Eq. (2.15) into Eq. (2.14) and using Eqs. (2.12) and (2.13) and equating matrix elements, we obtain self-consistent equations for the four unknown parameters ($\tilde{\omega}_n$, $\tilde{\Delta}_n$, $\tilde{H}_{Qn}$, and $\tilde{\Omega}_n$) which appear in the Green's function:

$$\tilde{\omega}_n-\omega_n=T\sum_m\int\frac{d^3k'}{(2\pi)^3}K_m^{-1}\{\tilde{\omega}_m[\tilde{\omega}_m^2+\tfrac{1}{2}(\epsilon_k^2+\epsilon_{k+Q}^2)+\tilde{\Delta}_m^2+\tilde{H}_{Qm}^2-\tilde{\Omega}_m^2]-2\tilde{\Omega}_m\tilde{H}_{Qm}\tilde{\Delta}_m\}g_{++} , \quad (2.17a)$$

$$\tilde{\Delta}_n-\Delta=T\sum_m\int\frac{d^3k'}{(2\pi)^3}K_m^{-1}\{\tilde{\Delta}_m[\tilde{\omega}_m^2+\tfrac{1}{2}(\epsilon_k^2+\epsilon_{k+Q}^2)+\tilde{\Delta}_m^2-\tilde{H}_{Qm}^2+\tilde{\Omega}_m^2]-2\tilde{\Omega}_m\tilde{\omega}_m\tilde{H}_{Qm}\}g_{-+} , \quad (2.17b)$$

$$\tilde{H}_{Qn}-H_Q=T\sum_m\int\frac{d^3k'}{(2\pi)^3}K_m^{-1}[-\tilde{H}_{Qm}(\tilde{\omega}_m^2-\epsilon_k\epsilon_{k+Q}-\tilde{\Delta}_m^2+\tilde{H}_m^2+\tilde{\Omega}_m^2)+2\tilde{\omega}_m\tilde{\Delta}_m\tilde{\Omega}_m]g_{--} , \quad (2.17c)$$

$$\tilde{\Omega}_n=T\sum_m\int\frac{d^3k'}{(2\pi)^3}K_m^{-1}[\tilde{\Omega}_m(\tilde{\omega}_m^2+\epsilon_k\epsilon_{k+Q}-\tilde{\Delta}_m^2-\tilde{H}_{Qm}^2-\tilde{\Omega}_m^2)+2\tilde{\omega}_m\tilde{\Delta}_m\tilde{H}_{Qm}]g_{+-} , \quad (2.17d)$$

where

$$K_m^{-1}=(\tilde{\omega}_m^2+\epsilon_k\epsilon_{k+Q}-\tilde{H}_{Qm}^2+\tilde{\Delta}_m^2-\tilde{\Omega}_m^2)^2-\epsilon_a^2(\tilde{\omega}_m^2+\tilde{\Delta}_m^2)+4(\tilde{\omega}_m\tilde{H}_{Qm}-\tilde{\Delta}_m\tilde{\Omega}_m)^2 . \quad (2.18)$$

Here we have omitted the arguments in $g_{\mu\nu}=g_{\mu\nu}(\vec{k}-\vec{k}';\omega_n-\omega_m)$. We define (for elastic impurities)

$$g_{\mu\nu}(\omega)=[U_1^2+\mu U_2^2(\langle S_x^2\rangle+\langle S_y^2\rangle+\nu\langle S_z^2\rangle)]\delta(\omega) , \quad (2.19)$$

and $\mu,\nu=\pm1$; here the omitted arguments in U_1^2 and U_2^2 are $(\vec{k}-\vec{k}')$. We have chosen H_Q to lie along the z axis. Note that in Eqs. (2.17a) and (2.17b), the thermal average $\langle S^2\rangle=\langle S_x^2\rangle+\langle S_y^2\rangle+\langle S_z^2\rangle$ appears. By contrast, Eqs. (2.17c) and (2.17d) depend on the quantity $\langle S_x^2\rangle+\langle S_y^2\rangle-\langle S_z^2\rangle$. The sign changes come about because of the commutation relations.

In order to include spin-fluctuation effects $U_2^2\times\langle S_x^2\rangle\delta(\omega)$ is replaced by $(J/2)^2\chi_{xx}(k-k',\omega)$ and similarly for the y and z components. Here χ is the time-ordered propagator for the localized spins. For notational simplicity throughout this section, we will present the formalism by explicitly including impurity effects only. The effects of spin fluctuations are discussed in detail in Sec. V.

Finally, Eqs. (2.17) must in turn be solved self-

consistently with the equations for Δ and the screened H_Q. These may be obtained from the Green's function $G(k,i\omega_n)$,

$$\Delta = -VT\sum_m \int \frac{d^3k'}{(2\pi)^3} \times \mathrm{Tr}[\rho_2\sigma_2 G(k,i\omega_m)] , \quad (2.20a)$$

$$H_Q = H_Q^0 - VT\sum_m \int \frac{d^3k'}{(2\pi)^3} \times \mathrm{Tr}[\tau_1\rho_3\sigma_3 G(k,i\omega_m)] . \quad (2.20b)$$

In general, the solution of these four [Eqs. (2.17)] simultaneous integral equations together with Eqs. (2.20) is exceedingly difficult. The easiest way to proceed is to chose a simple model for the Fermi surface (FS). In a previous Letter (L1) we presented our mean-field calculations for the AF superconductor using a spherical FS. When fluctuations and impurity effects are included, even this model is too difficult to handle. We resort, therefore, to the "quasi-3D" model suggested by Bilbro and McMillan[16] for charge-density waves in superconductors. It is assumed that in region I we have a 1D band so that $\epsilon_k \cong -\epsilon_{k+Q}$ for $k \cong -k_F$, while in region II, the small effect of $\tilde{H}_{Qn}$ and $\tilde{\Omega}_n$ are neglected. In our earlier work using the spherical FS, as we have noted above, the fraction of superconducting electrons γ in region I is related to $\omega_c/k_F Q$. In the "quasi-3D" model which we use in the following, we treat γ as an arbitrary parameter. Numerical results comparing the spherical FS model with the quasi-3D approximation can be obtained at the level of our coupled-mean-field theory. On this basis we will arrive at a reasonable estimate for γ.

In the "quasi-3D approximation," Eqs. (2.17) simplify considerably. We may perform the $\int d\vec{k}'$ and make use of the fact that $\epsilon_k = -\epsilon_{k+Q}$ in L1 to obtain

$$\tilde{\omega}_n - \omega_n = N(0)\sum_m \left[\gamma\left[\frac{(\tilde{\omega}_m+\tilde{\Omega}_m)}{2\lambda_m^+}+\frac{(\tilde{\omega}_m-\tilde{\Omega}_m)}{2\lambda_m^-}\right]+\frac{(1-\gamma)\tilde{\omega}_m}{(\tilde{\omega}_m^2+\tilde{\Delta}_m^2)^{1/2}}\right] g_{++}^0 , \quad (2.21a)$$

$$\tilde{\Delta}_n - \Delta = N(0)\sum_m \left[\gamma\left[\frac{(\tilde{\Delta}_m+\tilde{H}_{Qm})}{2\lambda_m^+}+\frac{(\tilde{\Delta}_m-\tilde{H}_{Qm})}{2\lambda_m^-}\right]+\frac{(1-\gamma)\tilde{\Delta}_m}{(\tilde{\omega}_m^2+\tilde{\Delta}_m^2)^{1/2}}\right] g_{-+}^0 , \quad (2.21b)$$

$$\tilde{H}_{Qn} - H_Q = -N(0)\sum_m \gamma\left[\frac{(\tilde{\Delta}_m+\tilde{H}_{Qm})}{2\lambda_m^+}-\frac{(\tilde{\Delta}_m-\tilde{H}_{Qm})}{2\lambda_m^-}\right] g_{--}^0 , \quad (2.21c)$$

$$\tilde{\Omega}_n = -N(0)\sum_m \gamma\left[\frac{(\tilde{\omega}_m+\tilde{\Omega}_m)}{2\lambda_m^+}-\frac{(\tilde{\omega}_m-\tilde{\Omega}_m)}{2\lambda_m^-}\right] g_{+-}^0 . \quad (2.21d)$$

Here $N(0)$ is the density of states at E_F and

$$\lambda_m^{\pm} = [(\tilde{\Delta}_m \pm \tilde{H}_{Qm})^2 + (\tilde{\omega}_m \pm \tilde{\Omega}_m)^2]^{1/2}/\pi T ,$$

and we have omitted the argument $(\omega_n - \omega_m)$ in $g_{\mu\nu}^0$. Here, $g_{\mu\nu}^0$ denotes the $l=0$ projection of $g_{\mu\nu}$. That is

$$g_{\mu\nu}^0(\omega_n) = \int_0^{2k_F} g_{\mu\nu}(q;\omega_n)\frac{q}{2k_F^2}dq ,$$

where $q = |\vec{k}-\vec{k}'|$ and both $\vec{k}$ and $\vec{k}'$ are presumed near k_F.

In this quasi-3D approximation we avoid the difficult issue of dealing with an anisotropic self-energy $\Sigma(\vec{k},i\omega_n)$ (which depends on the *direction* of $\vec{k}$). It may be seen from Eqs. (2.17) that because there are two angles which appear in the integral for Σ (that between $\vec{k}'$ and $\vec{Q}$, and that between $\vec{k}$ and $\vec{k}'$) that even for $\vec{k}$ and $\vec{k}'$ on the FS, the self-energy depends on $\vec{k}$. The solution of these equations requires the introduction of general spherical harmonics l in the coupling constant g, as well as in $\tilde{\Delta}_n$, etc. In the quasi-3D approximation the anisotropic effects only appear in region I. Furthermore, since region I is treated as a 1D system, only the $l=0$ projection enters into the expression for Σ. Without such an approximation it is doubtful that the problem could be solved. A numerical justification for this approximation is provided in Sec. IV.

Finally, the self-consistent equations for Δ and H_Q may be written in the quasi-3D approximation,

$$\Delta=N(0)V\sum_m\left[\gamma\left[\frac{(\tilde{\Delta}_m+\tilde{H}_{Qm})}{2\lambda_m^+}+\frac{(\tilde{\Delta}_m-\tilde{H}_{Qm})}{2\lambda_m^-}\right]+\frac{(1-\gamma)\tilde{\Delta}_m}{(\tilde{\omega}_m^2+\tilde{\Delta}_m^2)^{1/2}}\right], \tag{2.22a}$$

$$H_Q-H_Q^0=-N(0)V\sum_m\gamma\left[\frac{(\tilde{\Delta}_m+\tilde{H}_{Qm})}{2\lambda_m^+}-\frac{(\tilde{\Delta}_m-\tilde{H}_{Qm})}{2\lambda_m^-}\right]. \tag{2.22b}$$

A (numerical) solution of Eqs. (2.21) together with Eq. (2.22) thus yields all the necessary information about AF superconductors in the presence of spin fluctuations and impurities.

For the case of impurities which scatter elastically

$$N(0)g_{\mu\nu}(\omega)=\frac{1}{2}\left[\frac{1}{\tau_1}+\frac{\mu}{3\tau_2}(2+\nu)\right]\delta(\omega)\ , \tag{2.23}$$

where μ and $\nu=\pm1$.

$$\frac{1}{\tau_2}=4\pi c_2N(0)\,|\,U_2^0\,|^2S(S+1)\ ,$$

and

$$\frac{1}{\tau_1}=4\pi c_1N(0)\,|\,U_1^0\,|^2\ ,$$

$|\,U^0\,|^2$ is the $l=0$ projection of $|\,U\,|^2$; $c_{1,2}$ is the concentration of the appropriate impurities. In this case, we may readily perform the $\sum_m$ in Eqs. (2.21). For inelastic-scattering processes, such as those which arise from spin fluctuations, Eq. (2.21) do not simplify further.

III. APPLICATION TO ONE-DIMENSIONAL AF SUPERCONDUCTORS: NONMAGNETIC IMPURITY EFFECTS

We begin our analysis of Eqs. (2.21) by considering a 1D AF superconductor for which $\epsilon_k=-\epsilon_{k+Q}$ and $\gamma=1$ in Eqs. (2.21). This case is particularly informative because the effects of *nonmagnetic* elastically scattering impurities in AF superconductors can be cast into equations which are formally very similar to those found by Maki[8] [who, following Abrikosov and Gorkov (AG),[9] studied magnetic impurities in ordinary superconductors]. These lead to results in striking contrast to those found for nonmagnetic impurities in ordinary superconductors. Furthermore, Suzumura and Nagi[5] have extensively studied this limit for a pure AF superconductor and in the presence of an applied field. They correctly point out that even in zero external magnetic field, there is a first-order phase transition from the superconducting to the normal state as H_Q^0 is increased. However, by ignoring screening effects [see Eq. (2.22b)] they find this occurs at a critical value H_Q^0 which is about one half as large as that we obtain by including the effects of screening.

In the absence of magnetic impurities and considering only elastic scattering we can recombine Eqs. (2.21) (when we analytically continue to real frequencies) into a form which is similar to that of the AG theory,

$$u_\pm-\frac{\omega}{\Delta\pm H_Q}=\frac{1}{2}\frac{\zeta^\pm(u_\mp-u_\pm)}{(1-u_\mp^2)^{1/2}}\ , \tag{3.1}$$

where

$$u_\pm=\frac{\tilde{\omega}\pm\tilde{\Omega}}{\tilde{\Delta}\pm\tilde{H}_Q}\ . \tag{3.2a}$$

We define

$$\zeta^\pm\equiv\frac{1}{\tau_1}\frac{1}{\Delta\pm H_Q}\mathrm{sgn}(\Delta\mp H_Q)\ . \tag{3.2b}$$

Once the signs of $\zeta^\pm$ are chosen, Eqs. (3.1), together with the condition that $N_s(\omega)>0$, constrains the signs of $\mathrm{Re}(1-u_\pm^2)^{1/2}$. Alternative choices of the signs of $\zeta^\pm$ are clearly possible. However, they lead to unnecessary complications. We choose the $\pm$ signs in ζ in order to make $\zeta^\pm$ a smooth function of $1/\tau_1$. For this choice, both $\zeta^\pm$ have the sign of $(\Delta-H_Q)$.

It can be seen from Eq. (3.1) that scattering from *nonmagnetic* impurities affects the superconducting density of states $N_s(\omega)$,

$$N_s(\omega)\equiv\tfrac{1}{2}N(0)\mathrm{Im}\left[\frac{u_+}{(1-u_+^2)^{1/2}}+\mathrm{sgn}(\Delta-H_Q)\times\frac{u_-}{(1-u_-^2)^{1/2}}\right], \tag{3.3}$$

in the AF superconductors. Note that both contributions to the quantity in large parentheses must be positive [since they derive, respectively, from integrals like $\int d^3k\,\delta(E-E^{\pm}(k))$, where $E^{\pm}(k)$ are the quasiparticle energies which will be discussed in more detail below].[17]

For ordinary superconductors when only nonmagnetic impurities are present, Eq. (3.3) yields the BCS value

$$N_s(\omega)=N(0)\mathrm{Im}[\omega/(\Delta^2-\omega^2)^{1/2}]\ .$$

This result is commonly quoted as the "Anderson theorem." While nonmagnetic impurities in AF superconductors behave somewhat like magnetic impurities in usual superconductors, they cannot drive the system gapless in strictly 1D systems. Using Eqs. (3.1), it can be shown that a necessary condition for gaplessness is that $\zeta^-,\zeta^+<0$. In deriving this result one uses the fact that for $\zeta^{\pm}>0$, $\mathrm{Im}u^+$ and $\mathrm{Re}[(1-u_+^2)]^{1/2}$ must have the same signs (at $\omega=0$).[17] This together with the fact that $|\zeta^-|>\zeta^+|$ eliminates all possible gapless solutions of Eq. (3.1) for positive $\zeta^{\pm}$. Gaplessness in 1D systems thus requires that $H_Q>\Delta$. However, because a 1D system cannot[5] support an $H_Q>\Delta$, this inequality can never be satisfied. This result is not valid for a 3D superconductor, which may be driven gapless by nonmagnetic impurities, as shown in Sec. IV.

In the limit of a pure 1D AF superconductor $[(1/\tau_1)\to 0]$ it follows, from Eqs. (3.3) and (3.1), that

$$N_s(\omega)=\tfrac{1}{2}N(0)\mathrm{Im}\left[\frac{\omega}{[(\Delta+H_Q)^2-\omega^2]^{1/2}}+\frac{\omega}{[(\Delta-H_Q)^2-\omega^2]^{1/2}}\right]. \tag{3.4}$$

Thus, the density of states has two singularities at $\omega=|\Delta\pm H_Q|$. As (nonmagnetic) impurities are added these singularities become rounded peaks. In the limit $1/\tau_1\to\infty$, it can be shown that $N_s(\omega)$ is the usual BCS result. This can be seen by noting that a solution of Eq. (3.1) is $u_{\pm}\to\omega/\Delta$ in the limit $\zeta^{\pm}\to\infty$. Physically, this corresponds to the fact that the impurity (potential) scattering is sufficiently strong to smear out the antiferromagnetic gaps present in the normal-state band structure. The density of states, thus, becomes independent of the AF molecular field. It should be noted that $\tilde{H}_Q$, $\tilde{\Delta}$, $\tilde{\omega}$, etc., are *not* equal to H_Q, Δ, and ω, respectively. Interestingly, it follows from Eqs. (2.22) that $H_Q\to H_Q^0$ and $\Delta\to\Delta^{\mathrm{BCS}}$ in the limit $\tau_1\to 0$.

We have solved Eqs. (3.1) numerically using Newton's method and iterating down from high frequencies ω. The application is straightforward, although care must be exercised in choosing the correct branch of the square-root functions $(1-u_{\pm}^2)^{1/2}$. In order to obtain a positive $N_s(\omega)$, and continuous functions for $N_s(\omega)$, and $u_{\pm}$, the real parts of $(1-u_{\pm}^2)^{1/2}$ were initially positive (at high ω). We often then found $\mathrm{Re}(1-u_-^2)^{1/2}$ became negative as ω was decreased; $\mathrm{Re}(1-u_+^2)^{1/2}$ always remained positive for all frequencies.

$N_s(\omega)$ vs ω at $T=0$ is plotted in Fig. 1 for $\tau_1\omega_c=$(a) ∞, (b) 25, (c) 12.5, and (d) 2.5. Fixed values of $H_Q=0.01$ and $\Delta=0.013$ in units of ω_c were used in all the cases in Fig. 1. This value of H_Q is lower than would be expected experimentally[12] in order to maintain superconductivity in a 1D system. Because these 1D results are more of pedagogical value than of direct relevance to experimental systems, we did not solve for $N_s(\omega)$ self consistently with Δ and H_Q [i.e., using a fixed value of the coupling constant $N(0)V$]. Self-consistent results, however, are presented below for our quasi-3D model. As expected from Eq. (3.4), for the pure 1D superconductor, there are two divergences in $N_s(\omega)$ [see Fig. 1(a)] at $\omega=|\Delta\pm H_Q|$. As τ_1 decreases the peaks first round out (b) and then they merge into a single peak (c) which continues to sharpen (d), and thus become more BCS-like as τ_1 further decreases. These features are all in accord with the discussion presented above, based on analytical considerations.

IV. APPLICATION TO QUASI-3D AF SUPERCONDUCTORS: IMPURITY EFFECTS

A. Comparison between exact and quasi-3D results for pure systems

As discussed in Sec. II, the full solution of the six coupled integral equations needed to determine the Green's function G is exceedingly difficult in 3D systems. We, therefore adopt the "quasi-3D approximation" from which Eqs. (2.21) and (2.22) follow. As a check on this approximation and as a means of estimating the parameter γ, we now compare the results obtained for $N_s(\omega)$, $\Delta(T)$, and $H_c(T)$ (the thermodynamic critical field) in both the quasi-3D and the "exact" 3D calculations. For this comparison we use our coupled-mean-field

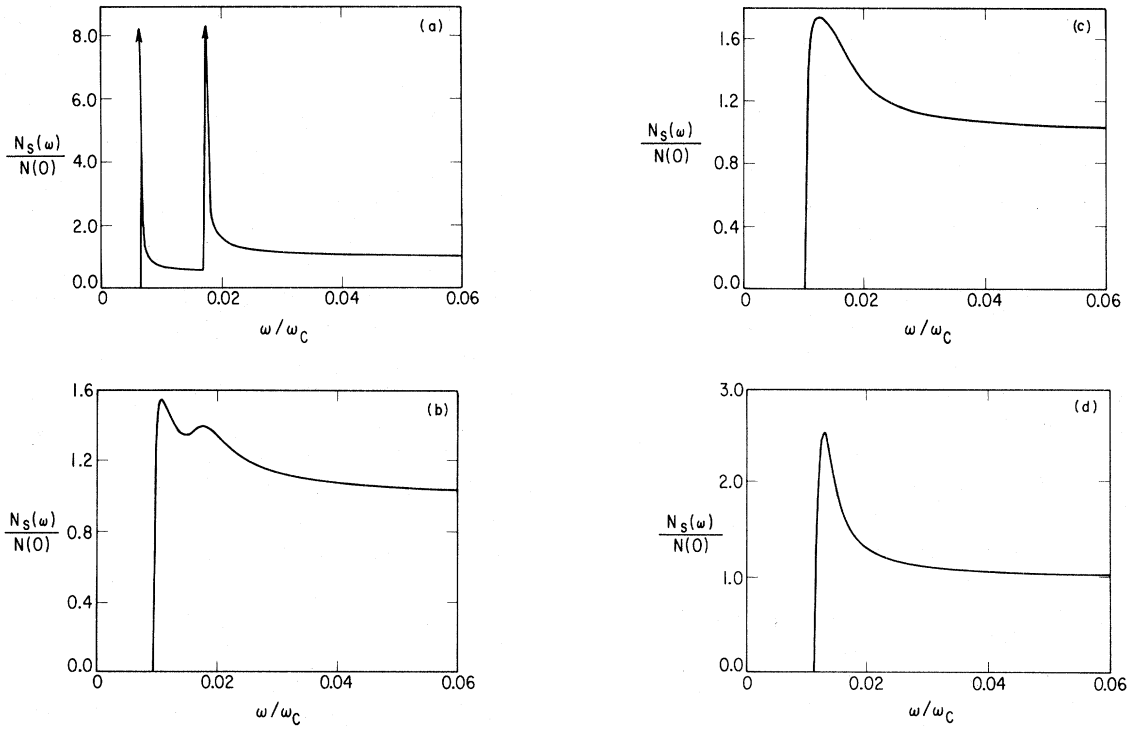

FIG. 1. $N_s(\omega)$ vs ω at $T=0$ for (a) $\tau_1\omega_c=\infty$, (b) 25.0, (c) 12.5, and (d) 2.5, in a 1D system.

theory with no impurities present. As in paper L1 in our "exact" 3D calculations we assume a spherical FS. In mean-field theory the electronic eigenenergies are given by[2]

$$E^{\pm}(k)=(\tfrac{1}{2}(\epsilon_k^2+\epsilon_{k+Q}^2)+\Delta^2+H_Q^2 \pm\tfrac{1}{2}\{(\epsilon_k^2-\epsilon_{k+Q}^2)^2+4H_Q^2[(\epsilon_k+\epsilon_{k+Q})^2+4\Delta^2]\}^{1/2})^{1/2},$$

from which the density of states,

$$N_s(\omega)\propto\int d^3k[\delta(\omega-E^+(k))+\delta(-E^-(k))], \tag{4.1}$$

may be readily evaluated. We applied a numerical technique in which a random mesh of 10^6 values of $\vec{k}$ (all with $k^2\leq 5\omega_c$) were summed over. For each value of k, $E^{\pm}(k)$ are determined and a histogram plot of $N_s(\omega)$ is generated. A smoothed out and normalized version of this histogram is presented in Figs. 2. We show $N_s(\omega)$ at $T=0$ for (a) $H_Q=0.1\omega_c$ and (b) $0.5\omega_c$. We chose $k_FQ=\omega_c$. This choice of Q is considerably smaller than would be expected experimentally; we use it here in order to emphasize the effects of the AF molecular

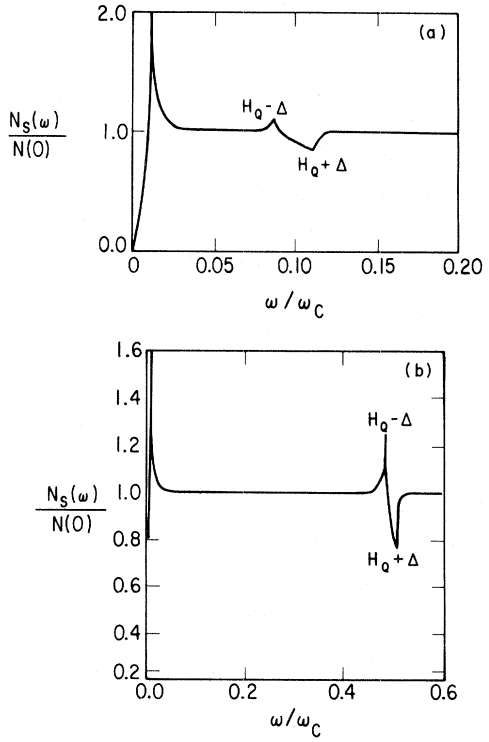

FIG. 2. $N_s(\omega)$ vs ω at $T=0$ for $H_Q=0.1\omega_c$ (a) and $0.5\omega_c$ (b), for pure superconductors.

field. Additionally we chose $\Delta=0.013\omega_c$ corresponding to the BCS value for Δ with $N(0)V=0.2$. It should be noted that there is a large peak in $N_s(\omega)$ for both figures at $\omega=\Delta$. This comes from those regions on the Fermi surface in which $|\epsilon_k-\epsilon_{k+Q}| >> H_Q$. Thus, the AF molecular field is relatively unimportant and Eq. (4.1) yields the BCS quasiparticle energies $(\epsilon_k^2+\Delta^2)^{1/2}$ and $(\epsilon_{k+Q}^2+\Delta^2)^{1/2}$ for values away from the magnetic Brillouin-zone boundary. However, for $|\epsilon_k-\epsilon_{k+Q}| \lesssim H_Q$, we do observe structure coming from the AF molecular field at $\omega\sim|\Delta\pm H_Q|$, as was seen in our 1D calculations. It is interesting to note that $N_s(\omega)$ rises rapidly from $\omega=0$, so that there is no true gap in $N_s(\omega)$ for these (rather physical) values of H_Q. Presumably for $H_Q<\Delta$, we would find a true gap in $N_s(\omega)$ obtained from our histogram approach. This case is relevant to temperatures near T_M. The density of states exhibits first a peak and then a dip at the frequencies $\omega=|\Delta\pm H_Q|$. We do not at present understand the origin of the "dip," which is different from what would be expected if region I were behaving like a strictly 1D system. However, we will show that once impurities are present, this subsidiary structure in $N_s(\omega)$ is of little consequence anyway.

These results should be compared with the $T=0$ plot of $N_s(\omega)$ for $\tau_1=\tau_2=\infty$, using our quasi-3D model. This is shown in Fig. 3 for $H_Q^0=0.1\omega_c$.[18] We choose the parameter $\gamma=0.02$ corresponding to 2% of the Fermi surface in region I. This choice for the value of γ was motivated by studying several T-dependent properties which are discussed below. For this case we solved self-consistently for Δ and H_Q using $N(0)V=0.2$ so that $\Delta=0.0127\omega_c$ and $H_Q=0.0988\omega_c$. Comparing Figs. 2 and 3 we see that both figures show the pronounced BCS peak at $\omega=\Delta$ and structure at $|\Delta\pm H_Q|$. However, in the quasi-3D model (with no impurities), $N_s(\omega)$ diverges at $|\Delta\pm H_Q|$, whereas in the exact numerical calculation (Fig. 2) there is only small structure at these additional frequencies. Note also that the quasi-3D model leads to a true gap in $N_s(\omega)$ which is not seen in Fig. 2. Hence, the quasi-3D model is generally less "gapless" than would be expected from an exact 3D calculation. The expected effects of impurities on the quasi-3D model are to weaken the subsidiary peaks at $|\Delta\pm H_Q|$ and to generally fill in the gap in the density of states at the Fermi energy (except in extremely dirty systems: $\tau_1\omega_c \lesssim 5.0$). In summary the quasi-3D model in the presence of impurities should be a reasonable approximation to an exact calculation for $N_s(\omega)$.

It is also useful to assess this approximation by looking at temperature-dependent quantities for pure superconductors. To do this we hose a T-dependent AF molecular field of the form $H_Q=H_Q(0)(1-T/T_M)^{1/2}$ and $T_M=\frac{1}{3}T_c^{\rm BCS}$, where T_M is the magnetic ordering temperature and $N(0)V=0.2$. The T dependence of Δ and H_c^2 were illustrated in paper L1 using our "exact" 3D calculation. In Figs. 4 and 5 we plot these quantities (for slightly different parameters than in paper L1) in the exact 3D (solid lines) and quasi-3D approximation (dashed and dotted-dashed lines). We fixed the value of $H_Q(0)$ at $0.1\omega_c$ in curves b and c which is slightly below the experimental value[18] and varied the parameter k_FQ/ω_c or γ. The solid lines in Fig. 4 plot Δ vs T for (a) the BCS limit, (b) $k_FQ/\omega_c=3.0$, and (c) $k_FQ/\omega_c=0.2$. The dashed line is for $\gamma=0.02$ and the dotted-dashed line is for $\gamma=0.01$. These small values of γ yield semiquantitative agreement for $\Delta(T)$ with the values obtained

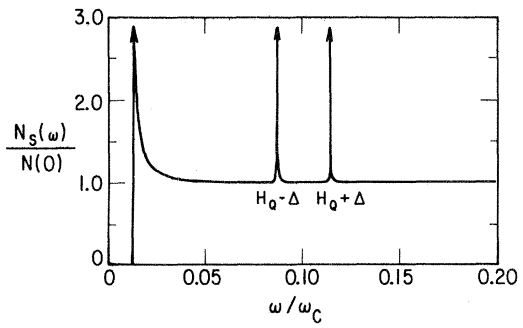

FIG. 3. $N_s(\omega)$ vs ω in quasi-3D model for a pure superconductor.

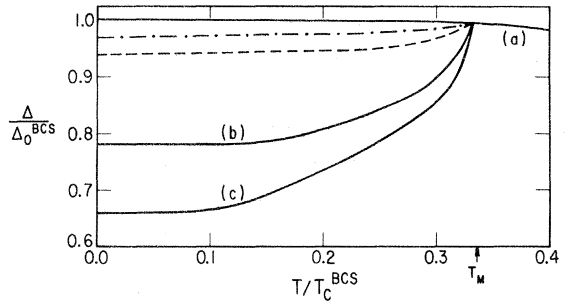

FIG. 4. Δ vs T for "exact" (solid lines) and quasi-3D [dashed ($\gamma=0.02$) and dotted-dashed ($\gamma=0.01$) lines] model. Solid lines correspond to (a) BCS limit, (b) $k_FQ/\omega_c=3.0$, and (c) $k_fQ/\omega_c=2.0$

in the exact 3D calculations with a reasonable choice for $k_F Q/\omega_c$. Since even the latter parameter is not known accurately from experiment we did not make any attempt to fit our more *ad hoc* parameter γ exactly to any given theoretical curve. It is clear from the figure that $\gamma \sim 0.01$ or 0.02 is required to get reasonable agreement between the exact and quasi-3D calculations.

Figure 5 illustrates the behavior of the thermodynamic field $H_c^2(T)$. This parameter corresponds to the free-energy difference between the superconducting and normal states. The results obtained for a pure 3D superconductor, treated "exactly" as in paper L1 are indicated by the solid lines for (a) the BCS limit, (b) $k_F Q/\omega_c = 3.0$, and (c) $k_F Q/\omega_c = 2.0$. We took $H_Q(0) = 0.1\omega_c$ in curves *b* and *c*. The dashed line corresponds to $\gamma = 0.02$ and the dotted-dashed line to $\gamma = 0.01$ (with the same value of $H_Q(0) = 0.1\omega_c$). Again these values of γ are in semiquantitative agreement with those obtained by our more exact procedure. In summary, we deduce from Figs. 4 and 5 that a reasonable estimate of $\gamma \cong 0.02$. We also note that for somewhat larger values of γ with $N(0)V = 0.2$ and $H_Q(0) = 0.1\omega_c$, we find that the system undergoes a first-order phase transition to the normal state at low T, as found previously[5] for a strictly 1D system. That such a small region I is required to avoid the first-order transition is presumably an artifact of the quasi-3D model in which all electrons in region I feel the effects of the magnetic molecular field to a great extent. We see no evidence for a first-order transition for reasonable values of H_Q in our more exact 3D calculations.[2]

B. Impurity effects at $T=0$

In this section we discuss the effects of magnetic and nonmagnetic impurities in $N_s(\omega)$, $\tilde{\Delta}(\omega)$, $\tilde{H}_Q(\omega)$, etc., at zero temperature. These are calculated within the quasi-3D model. Throughout we assume $\gamma = 0.02$ and $H_Q^0/\omega_c = 0.1$ with $N(0)V = 0.20$. The latter two parameters are believed to be reasonable for the AF superconductors.[18]

We do not exhibit results for $N_s(\omega)$ at finite T, since this quantity behaves as would be expected from its $T=0$ values and the T dependence of Δ. In the quasi-3D model $N_s(\omega)$ is given by

$$N_s(\omega) = N(0)\left[\frac{1}{2}\mathrm{Im}\left[\frac{(\tilde{\omega}+\tilde{\Omega})\gamma}{[(\tilde{\Delta}+\tilde{H}_Q)^2-(\tilde{\omega}+\tilde{\Omega})^2]^{1/2}}+\frac{(\tilde{\omega}-\tilde{\Omega})\gamma}{[(\tilde{\Delta}-\tilde{H}_Q)^2-(\tilde{\omega}-\tilde{\Omega})^2]^{1/2}}+\frac{2(1-\gamma)\tilde{\omega}}{(\tilde{\Delta}^2-\tilde{\omega}^2)^{1/2}}\right]\right], \tag{4.2}$$

where $\tilde{\omega}$, $\tilde{\Delta}$, $\tilde{\Omega}$, and $\tilde{H}_Q$ are functions of ω. We solved for these functions using Eqs. (2.21) and Newton's method. We started from high frequency, making reasonable guesses for their solutions and then decreased ω, using the four values (for $\tilde{\omega}$, $\tilde{\Delta}$, $\tilde{\Omega}$, and $\tilde{H}_Q$) obtained at the previous frequency as an initial guess.

In Fig. 6 is plotted $N_s(\omega)$ vs ω for a superconductor with only nonmagnetic impurities ($\tau_2 \to \infty$) for (a) $\tau_1^{-1} = 0.004$, (b) $\tau_1^{-1} = 0.016$, (c) $\tau_1^{-1} = 0.4$, and (d) $\tau_1^{-1} = 2.0$, all in units of ω_c. In order to have a reference point with which to compare these figures, we estimate that $\tau_1 \sim 10^{-11}$ to 10^{-12} sec in the cleanest ternary compounds. For $\omega_c \sim 10^{-13}$ sec^{-1}, this yields $\tau_1^{-1} \sim 0.01$ to 0.1 in units of ω_c. The self-consistently determined values of Δ/ω_c and H_Q/ω_c are (a) 0.0128 and 0.0988, (b) 0.0124 and 0.0991, (c) 0.0130 and 0.0994, and (d) 0.0133 and 0.0998. Figure 6(a) has a well-defined gap, a sharp peak at Δ and smaller

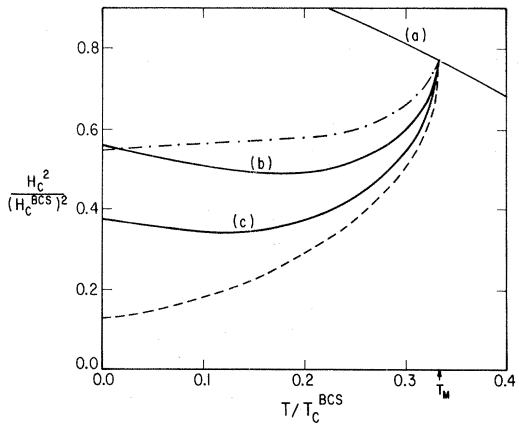

FIG. 5. H_c^2 vs T for exact (solid lines) and quasi-3D [dashed ($\gamma = 0.02$) and dotted-dashed ($\gamma = 0.01$) lines] model. Solid lines correspond to (a) BCS limit, (b) $k_F Q/\omega_c = 3.0$, and (c) $k_F Q/\omega_c = 2.0$.

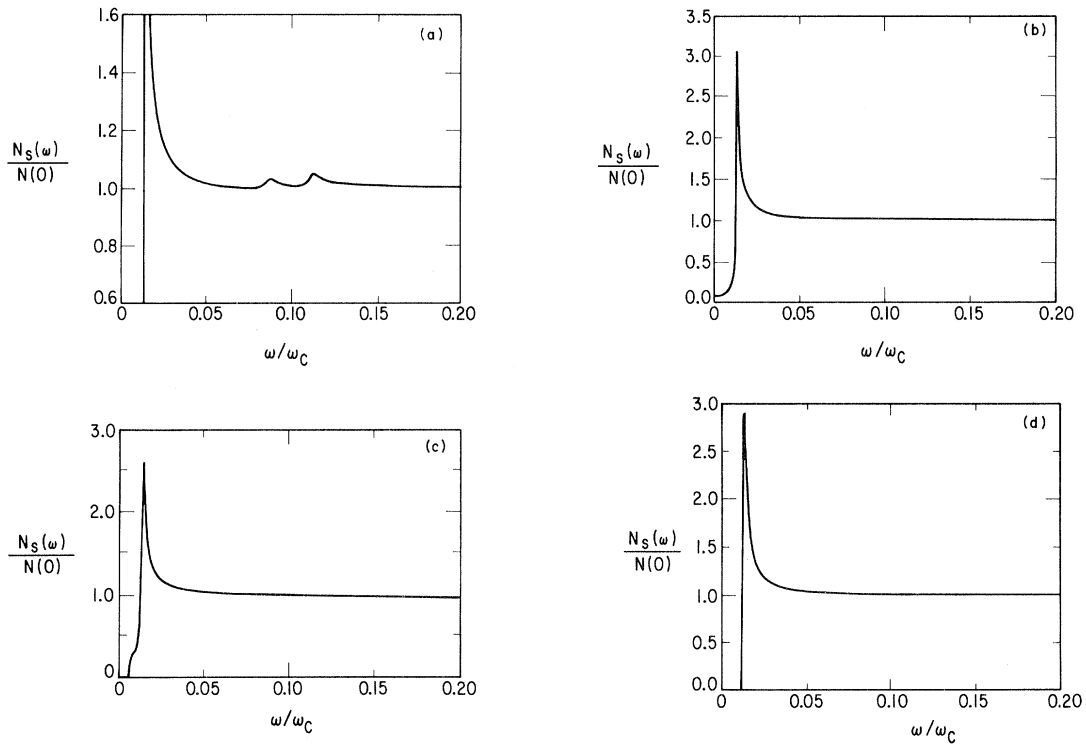

FIG. 6. $N_s(\omega)$ vs ω for $\tau_2 \rightarrow \infty$ and (a) $\tau_1^{-1}=0.004$, (b) $\tau_1^{-1}=0.016$, (c) $\tau_1^{-1}=0.4$, and (d) $\tau_1^{-1}=2.0$, all in units of ω_c.

peaks at $|\Delta \pm H_Q|$. These are rounded relative to the case of a pure superconductor, as was seen in the earlier 1D calculations. As the nonmagnetic impurity concentration increases we see the filling in of the gap and the disappearance of the subsidiary peaks. Figure 6(b) shows that nonmagnetic impurities can induce gaplessness in a magnetic superconductor. Figures 6(c) and 6(d) show that as the impurity concentration increases still further the system regains its gap and becomes more BCS-like, as was demonstrated rigorously to be the case for our 1D system.

Figures 7 illlustrate the behavior of $N_s(\omega)$ when magnetic impurities are present for (a) $\tau_1^{-1}=0$, $\tau_2^{-1}=0.002$, (b) $\tau_1^{-1}=0$, $\tau_2^{-1}=0.0045$, (c) $\tau_2^{-1}=0.004$, $\tau_1^{-1}=0.20$, and (d) $\tau_2^{-1}=0.004$, $\tau_1^{-1}=0.4$, all in units of ω_c. The self-consistent values of Δ and H_Q (in units of ω_c) are, respectively, (a) 0.011, 0.0988, (b) 0.0125, 0.0992, (c) 0.0083, 0.0991, and (d) 0.0081, 0.0994. As for a usual (nonmagnetic superconductor), for small τ_2^{-1} there is a gap in $N_s(\omega)$. However, in the case of the AF superconductor, there are also two additional peaks at $\omega=|\Delta \pm H_Q|$. This is seen in Fig. 7(a). Figure 7(b) shows that as τ_2^{-1} increases the gap narrows and the subsidiary peaks also weaken. We found that as in the nonmagnetic superconductors,[8] gapless superconductivity sets in at about $\tau_2^{-1} \sim \Delta$ and the system was driven normal for $\tau_2^{-1} \sim \frac{1}{2}\Delta_0^{\mathrm{BCS}} \equiv \frac{1}{2}\Delta^{\mathrm{BCS}}(T=0)$. Interestingly enough, even for a gapless superconductor, the subsidiary peaks do not completely disappear. In fact at $\tau_2^{-1}=0.0064\omega_c$ the secondary peaks (which are essentially unresolvable) reach a higher value of $N_s(\omega)$ than does the BCS peak. The effects of superposing potential-scattering impurities on top of magnetic impurities are quite dramatic. These are illustrated in Figs. 7(c) and 7(d). For small additional concentration of nonmagnetic impurities the superconductor becomes gapless [Fig. 7(c)]. Increasing τ_1^{-1} still further, while keeping τ_2^{-1} a constant, results in a return of the gap and more BCS-like behavior. This is similar to what was seen in Figs. 6 for $\tau_2^{-1}=0$; as τ_1^{-1} grows, impurity states first fill in the gap in the density of states. Then increasing τ_1^{-1} still further, the system becomes more BCS-like.

For completeness we have plotted the real and imaginary parts of the frequency-dependent (renormalized) self-energy parameters $\tilde{\omega}$, $\tilde{\Delta}$, $\tilde{H}_Q$, and $\tilde{\Omega}$

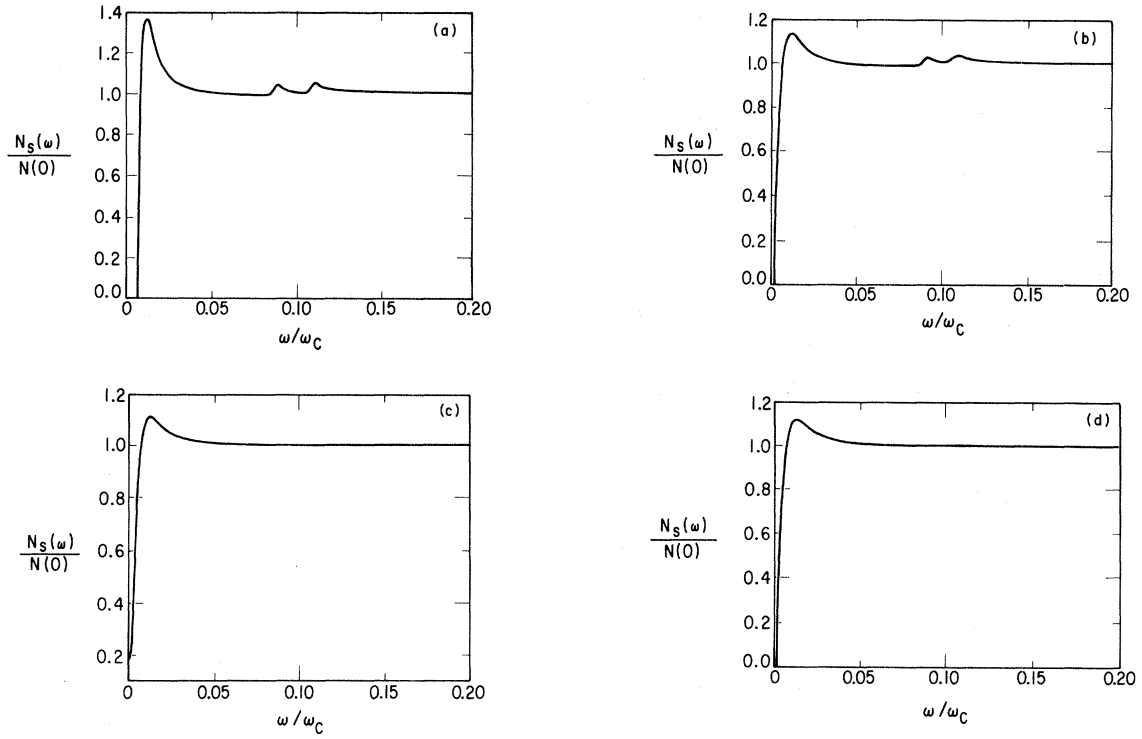

FIG. 7. $N_s(\omega)$ vs ω for (a) $\tau_1^{-1}=0$, $\tau_2^{-1}=0.002$, (b) $\tau_1^{-1}=0$, $\tau_2^{-1}=0.0045$, (c) $\tau_2^{-1}=0.004$, $\tau_1^{-1}=0.20$, and (d) $\tau_1^{-1}=0.4$, $\tau_2^{-1}=0.004$, all in units of ω_c.

for $\tau_1^{-1}=0.004\omega_c$ and $\tau_2^{-1}=0$ (Figs. 8), and $\tau_2^{-1}=0.004\omega_c$, $\tau_1^{-1}=0$ (Figs. 9). As seen from Figs. 8(b) and 9(b) most of the structure in $\tilde{\Delta}$ is below the gap frequency. While $\tilde{\omega}$ shows virtually no structure for the case of magnetic impurities [Fig. 9(a)], when nonmagnetic impurities are present [Fig. 8(a)] there are features which appear below the gap. For both Figs. 8(c) and 9(c), $\tilde{H}_Q$ is nearly constant with an almost vanishing imaginary part. A rather detailed structure appears in $\tilde{\Omega}$ at frequencies away from the gap frequency. However, it should be noted that this is on a scale which is about 3 orders of magnitude smaller than Δ and 4 orders of magnitude smaller than H_Q.

C. Finite-temperature effects

In this section we numerically compute Δ and H_c^2 as a function of temperature in AF superconductors, when impurities are present. While it is probably difficult to measure the experimental values of Δ, it is nevertheless enlightening to study the effects of impurities on the superconducting order parameter.[19]

The self-consistent equations for Δ and H_Q obtained from Eqs. (2.22), are approximately given by

$$\Delta=\frac{N(0)V}{2}\int_0^{\omega_c'}d\omega\,\mathrm{Im}\left[\gamma\left[\frac{\tilde{\Delta}+\tilde{H}_Q}{\lambda^+}+\frac{\tilde{\Delta}-\tilde{H}_Q}{\lambda^-}\right]+\frac{2(1-\gamma)\tilde{\Delta}}{(\tilde{\Delta}^2-\tilde{\omega}^2)^{1/2}}\right]\times\tanh\frac{\beta\omega}{2}\,, \tag{4.3a}$$

$$H_Q=H_Q^0-\frac{N(0)V}{2}\int_0^{\omega_c'}d\omega\,\mathrm{Im}\left[\gamma\left[\frac{\tilde{\Delta}+\tilde{H}_Q}{\lambda^+}-\frac{(\tilde{\Delta}-\tilde{H}_Q)}{\lambda^-}\right]\right]\times\tanh\frac{\beta\omega}{2}\,, \tag{4.3b}$$

where $\lambda^{\pm}=[(\tilde{\Delta}\pm\tilde{H}_Q)^2-(\tilde{\omega}\pm\tilde{\Omega})^2]^{1/2}$. Here we have analytically continued Eqs. (2.22) to the real axis and replaced the Matsubura sum by an integral over frequency. The integration cutoff in these equations, ω_c' is approximately (Ref. 10) ω_c

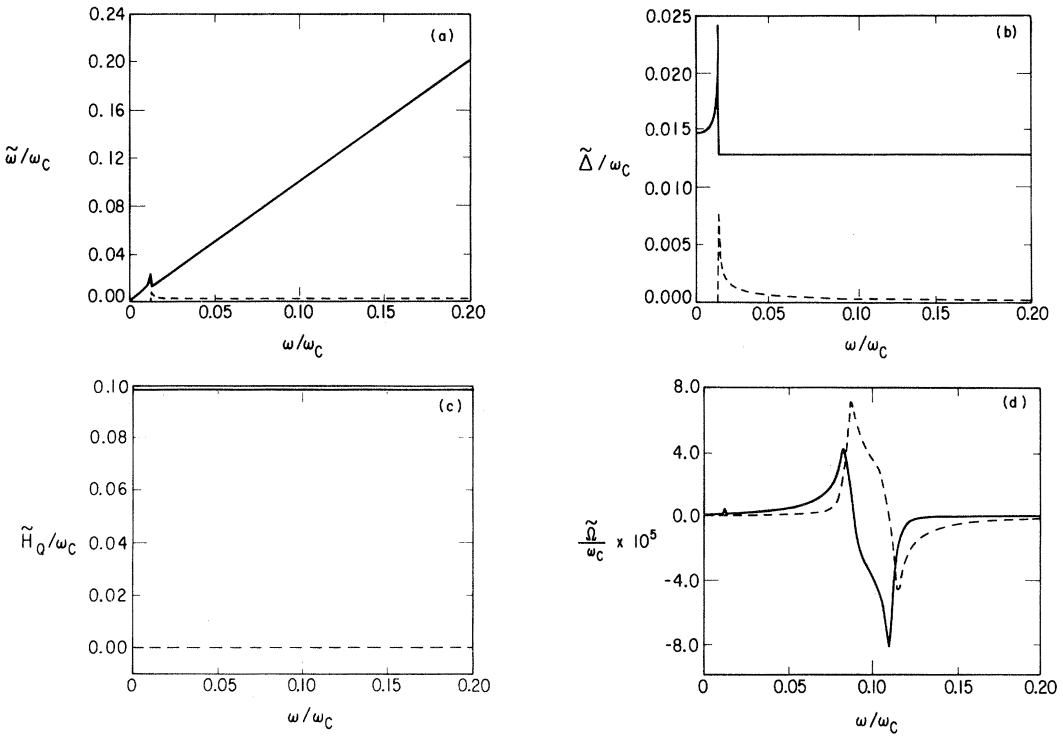

FIG. 8. Real (solid lines) and imaginary (dashed lines) parts of $\tilde{\omega}$ [in (a)], $\tilde{\Delta}$ [in (b)], $\tilde{H}_Q$ [in (c)], and $\tilde{\Omega}$ [in (d)], for $\tau_1^{-1}=0.004\omega_c$ and $\tau_2^{-1}=0$.

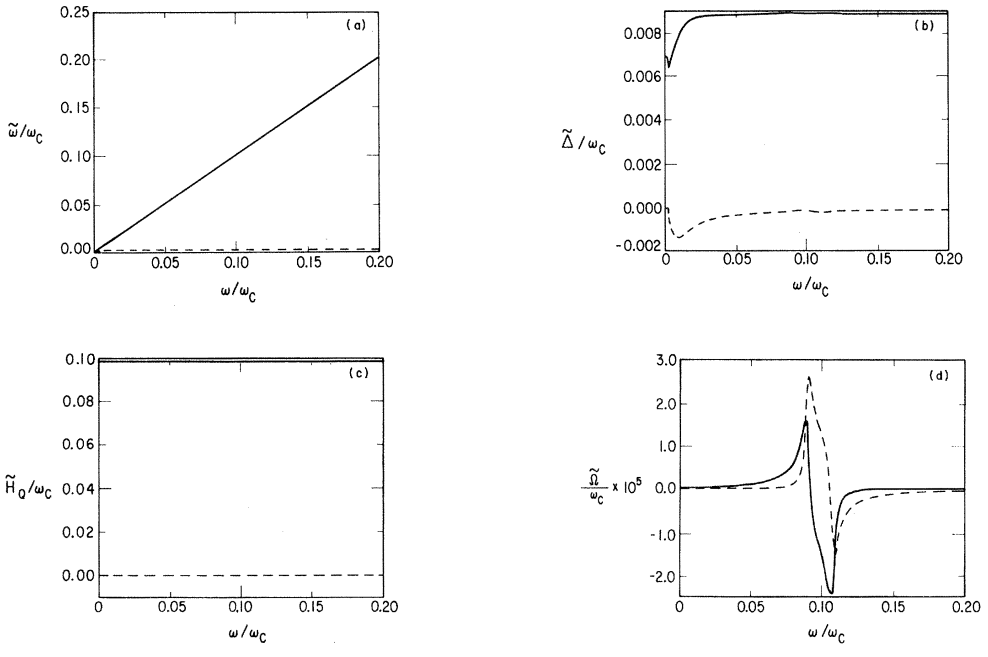

FIG. 9. Real (solid lines) and imaginary (dashed lines) parts of $\tilde{\omega}$ [in (a)], $\tilde{\Delta}$ [in (b)], $\tilde{H}_Q$ [in (c)], and $\tilde{\Omega}$ [in (d)], for $\tau_1^{-1}=0$, $\tau_2^{-1}=0.004\omega_c$.

to within corrections of order the maximum of $(H_Q/\omega_c)^2$ and $(\Delta/\omega_c)^2$. Since these are both numbers of order (0.01) or less, these corrections will be ignored and we take $\omega_c'=\omega_c$. We have verified that our solution to the above equations reproduces the usual BCS result at low temperatures. When $H_Q^0=0$, it yields good agreement with the low-temperature values[8] of Δ for the case of a nonmagnetic superconductor with magnetic impurities.

In Fig. 10 is plotted the gap parameter Δ as a function of temperature $T/T_c^{\rm BCS}$ for (a) $\tau_2^{-1}=0$ and $\tau_1^{-1}=0.16\omega_c$, and (b) $\tau_1^{-1}=0$ and $\tau_2^{-1}=0.004\omega_c$. As before, we take $H_Q=0.1\omega_c(1-T/T_M)^{1/2}$ and $T_M=\frac{1}{3}T_c^{\rm BCS}$. Figure 10(a) shows that for nonmagnetic impurities the shape of Δ is similar to that of a pure AF superconductor (see Fig. 4). There is a cusp at the magnetic ordering temperature. The decrease in Δ as T decreases below T_M is due to the increase in the AF molecular field. For $T>T_M$, Δ assumes the BCS value. For magnetic impurities, Δ vs T has two maxima, one at $T\cong 0$ and another at $T=T_M$. The differences in Figs. 10(a) and 10(b) are due to the fact that the superconducting transition temperature, $T_c=0.55T_c^{\rm BCS}$, is considerably smaller for the case of magnetic impurities. Thus, Δ falls off rapidly below T_M as T increases; even though H_Q is decreasing with increasing T, effects of this molecular field are not sufficiently strong to counterbalance the tendency of Δ to decrease with increasing T. In the immediate vicinity of the magnetic ordering temperature, however, there is a small cusp in Δ due to the sudden turning on of the molecular field. For $T>T_M$, Δ assumes the Abrikosov-Gorkov value.

To calculate the thermodynamical critical field, we follow the formalism of Skalski *et al.*[10] This approach is more tractable than numerical coupling-constant integration techniques. We have for the difference in free energies of the superconducting and normal states,

$$F_s-F_N=-\int_0^{\omega_c'}d\omega[N_s(\omega)-N_H(\omega)]2\omega\tanh\frac{\beta\omega}{2}+\frac{\Delta^2}{V}-N(0)\Delta^2$$
$$-4\beta^{-1}\int_0^{\omega_c'}d\omega[N_s(\omega)-N_H(\omega)][\ln(1+e^{-\beta\omega})+\beta\omega/(e^{\beta\omega}+1)]\,. \tag{4.4}$$

Using $N_s(\omega)$, the superconducting density of states we computed earlier, we may then obtain $-H_c^2=8\pi(F_s-F_N)$. Here, $N_H(\omega)=\lim_{\Delta\to 0}N_s(\omega)$. Note that this quantity differs from $N(0)$ due to the antiferromagnetic molecular field H_Q. We find $N_H(\omega)$ has a small peak at $\omega=H_Q$ for low to moderate impurity concentrations.

In Figs. 11(a) and 11(b) are plotted H_c^2 as a function of temperature for (a) $\tau_1^{-1}=0.16\omega_c$, $\tau_2^{-1}=0$, and (b) $\tau_1^{-1}=0$, $\tau_2^{-1}=0.004\omega_c$. These are the same parameters as used in Figs. 10(a) and 10(b). For the case of potential scattering only [Fig. 11(a)], we see a rather complex structure. However, it should be noted that the variations of H_c^2 with T are on a scale small compared to H_c^2. In both Figs. 11, there is a sharp drop in H_c^2 with decreasing T at T_M, i.e., when the molecular field turns on. In Fig. 11(a) there are two opposing trends in H_c^2: a general tendency to increase as T decreases, as in BCS theory, and the reflection of the decrease in Δ with decreasing T [seen in Fig. 10(a)]. This leads to a low-temperature maximum. In Fig. 11(b) the fact that Δ increases with decreasing T [see Fig. 10(b)] causes a rapid increase in H_c^2 with decreasing T. This curve looks qualitatively in agreement

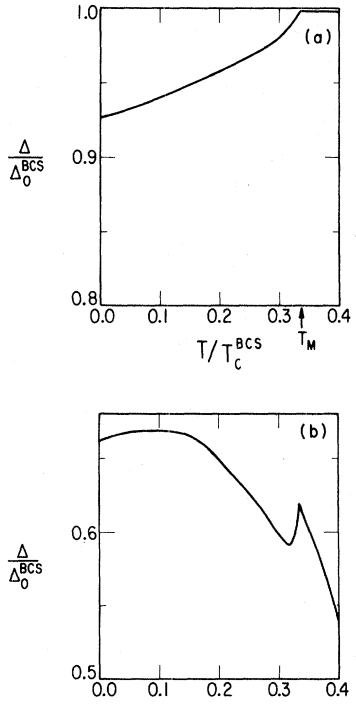

FIG. 10. Δ vs T for (a) $\tau_2^{-1}=0$, $\tau_1^{-1}=0.16\omega_c$; and (b) $\tau_1^{-1}=0$, $\tau_2^{-1}=0.004\omega_c$ where $\Delta_0^{\rm BCS}\equiv\Delta^{\rm BCS}(T=0)$.

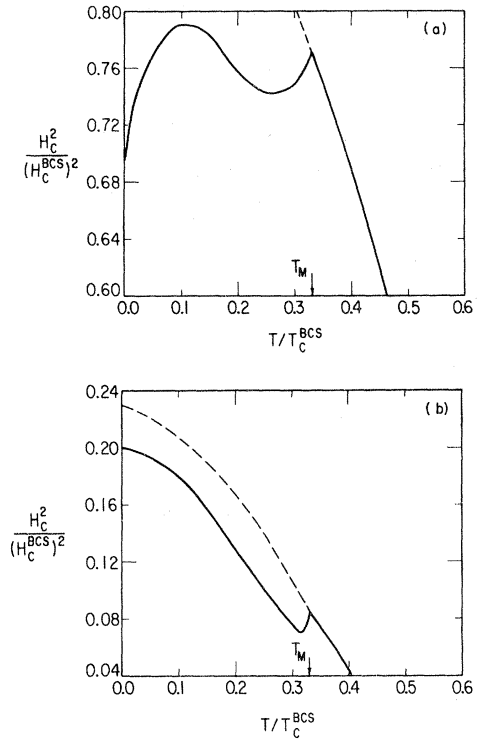

FIG. 11. H_c^2 vs T for (a) $\tau_2^{-1}=0$, $\tau_1^{-1}=0.16\omega_c$; and (b) $\tau_1^{-1}=0$, $\tau_2^{-1}=0.004\omega_c$.

with what is observed experimentally[20] for H_{c2}. For completeness, we have indicated the expected behavior of H_c^2 for the case $H_Q^0=0$ by the dashed lines. This projection of the nonmagnetically ordered state leads to the BCS curve in Fig. 11(a) and the usual[8] magnetic-impurity curve in Fig. 11(b). Note that in the latter case $T_c \neq T_c^{BCS}$.

In summary, it can be noted from Figs. 11(a), 11(b), and 4 that the temperature dependence of H_c^2 is quite sensitive to impurity effects. This is likely to be true for the parameter H_{c2} as well. Furthermore, because longitudinal spin-fluctuation effects are similar to those of magnetic impurities, we expect that a more realistic prediction for the behavior of H_c^2 in the AF superconductors is that shown in Fig. 11(b).

V. SPIN-FLUCTUATION EFFECTS

Equations (2.21) are readily generalized to the case where spin fluctuations are present. We may carry out the sum over frequencies ω_m using the spectral representation of the propagator χ to obtain,[21] for example,

$$\tilde{\omega}-\omega=\int_{-\infty}^{\infty}d\omega'\int_0^{\infty}d\nu\,\mathrm{Im}\left[\gamma\left[\frac{\tilde{\omega}'+\tilde{\Omega}'}{2\lambda'_+}+\frac{\tilde{\omega}-\Omega'}{2\lambda'_-}\right]+\frac{(1-\gamma)\tilde{\omega}'}{(\tilde{\Delta}^2-\tilde{\omega}^2)^{1/2}}\right]\times K(\omega,\omega',\nu)\alpha^2F(\nu)\ , \tag{5.1}$$

where $\tilde{\omega}\equiv\tilde{\omega}(\omega')$, etc., and

$$K(\omega,\omega',\nu)=\frac{f(-\omega')+n(\nu)}{\omega'+\nu-\omega}+\frac{f(\omega')+n(\nu)}{\omega'-\nu-\omega}\ . \tag{5.2}$$

Here,

$$\lambda'_{\pm}=[(\tilde{\Delta}'\pm\tilde{H}'_Q)^2+(\tilde{\omega}'\pm\tilde{\Omega}')^2]^{1/2}\ . \tag{5.3}$$

The equations for $\tilde{\Omega}$, $\tilde{\Delta}$, and $\tilde{H}_Q$ are similar. The parameter $\alpha^2F(\nu)$, which is the effective coupling constant times magnon density of states, is

$$\alpha^2F(\nu)\equiv N(0)J^2\int_0^{2k_F}\phi(q)B(q,\nu)d^3q\ , \tag{5.4}$$

where $B(q,\nu)$ is the Fourier transform of $\langle[S_i(t),S_j(0)]\rangle$ and is thus related to χ by the spectral representation. Here $\phi(q)$ is the joint density of states of conduction electrons[6] whose wave vectors are separated by q. For a spherical Fermi surface $\phi\propto 1/q$, so that

$$\alpha^2F(\nu)\equiv N(0)J^2\int_0^{2k_F}\frac{qdq}{2k_F^2}B(q,\nu)\ . \tag{5.5}$$

Thus $\alpha^2F(\nu)$ is related to the $l=0$ projection of $B(q,\nu)$, similar to what was assumed for the case of elastic impurities in Sec. II and in previous work on spin-glass superconductors.[21,22] Strictly speaking, we have implicitly assumed the Fermi surface to be spherical in deriving Eq. (5.1). However, in what follows it is informative to view $\alpha^2F(\nu)$ as a general function which depends on an arbitrary $\phi(q)$.

Equations analogous to Eqs. (2.21b)–(2.21d) for the case of spin-fluctuation scattering may be readily written down using Eq. (5.1). The quanity in large brackets in Eq. (5.1) is replaced by that in Eqs. (2.21b)–(2.21d) (analytically continued to real frequencies) to get the appropriate equation for $\tilde{\Delta}-\Delta$, $\tilde{H}_Q-H_Q$, and $\tilde{\Omega}-\Omega$, respectively. The kernel $K(\omega,\omega',\nu)$ is the same in all four equations.

The quantity $\alpha^2F(\nu)$ appears in the equations for $\tilde{\omega}-\omega$ and $\tilde{\Delta}-\Delta$, while $1/3\alpha^2F(\nu)$ appears in the expression for $\tilde{H}_Q-H_Q$ and $\tilde{\Omega}$. This factor of $\frac{1}{3}$ derives from the facts that (i) we assume[23] an isotropic $\chi\equiv\frac{2}{3}\chi_\perp+\frac{1}{3}\chi_{||}$, and (ii) that [from Eq. (2.19)] that different combinations of the x, y, and z components of χ appear in the self-energy contributions.

The detailed form of $\alpha^2F(\nu)$ for antiferromagnetic spin fluctuations is not known for the ternary compounds. On the basis of the *phonon* analog of this quantity (called α^2F in the literature) we expect that there are in general three peaks in the "magnon" α^2F; a diffuse peak at $\omega=0$ (corresponding to longitudinal fluctuations) and spin-wave peaks at $|\omega|=\omega_S\cong T_M$ (corresponding to the transverse fluctuations). The relative weight of the elastic peak grows with increasing temperature, whereas the inelastic peak becomes weaker. The simplest model[24] consistent with this picture is to take for $T\lesssim T_M$,

$$\alpha^2F(\nu)=\{S(S+1)T/T_M\delta(\nu)+\tfrac{1}{2}S(1-T/T_M)\times[\delta(\nu-\omega_s)+\delta(\nu+\omega_s)]\}\times\frac{n}{2}N(0)J^2(1-e^{-\beta|\nu|}) . \quad (5.6)$$

Here, n is the density of rare-earth spins. Above T_M we assume that $\alpha^2F(\nu)$ is given by its value at T_M, which is just the Abrikosov-Gorkov[9] expression for scattering from noninteracting spins,

$$\alpha^2F(\nu)=J^2\frac{n}{2}S(S+1)(1-e^{-\beta\nu})\delta(\nu) . \quad (5.7)$$

Note that the elastic peak has zero weight at $T=0$ in an antiferromagnet; this is in contrast to the situation in a spin glass,[25] where there is always spin-disorder scattering at any temperature. It should also be noted that elastically scattering impurities will contribute a (constant in temperature) $\delta(\nu)$ term to the scattering function.

In fact, we may readily superpose impurity on top of spin-fluctuation effects. This leads to $[\alpha^2F(\nu)]_{\rm imp}$,

$$[\alpha^2F(\nu)]^{\mu\mu'}_{\rm imp}=\frac{\beta\nu\delta(\nu)}{2\pi}\left[\frac{1}{\tau_1}+\frac{\mu}{3\tau_2}(2+\mu')\right]$$
$$\mu\mu'=\pm1 . \quad (5.8)$$

The equations for $\tilde{\omega}-\omega$ and $\tilde{\Delta}-\Delta$ follow from Eq. (5.1) and its analog by using the combination

$$[\alpha^2F(\nu)]_{\rm tot}\equiv\alpha^2F(\nu)+[\alpha^2F(\nu)]_{\rm imp} .$$

The $\mu\mu'$ sign conventions are as in Eqs. (2.21).

We have numerically solved the four coupled equations for $\tilde{\omega}$, $\tilde{H}_Q$, $\tilde{\Delta}$, and $\tilde{\Omega}$ in order to obtain $N_s(\omega)$ in the presence of spin fluctuations. Because of the complexity of Eq. (5.1) and its analogs, we did not solve self-consistently for Δ and H_Q. Rather, we have fixed Δ and H_Q, and solved iteratively for the quantities of interest.

Our numerical results for $N_s(\omega)$ are plotted in Figs. 12 and 13 for $S=\frac{5}{2}$, $\gamma=0.02$, $\Delta=0.01\omega_c$, and $H_Q^0=0.10\omega_c$. Figures 12 correspond to a superconductor with magnetic impurities at $T=0$. The spin-wave frequency $\omega_s=0.0025\omega_c$. In this case $(\tau_2)^{-1}=0.0057\omega_c$ and $\tau_s^{-1}=0.016\omega_c$. Here, the spin-flip-scattering time from the rare-earth atoms is

$$\tau_s^{-1}\equiv\pi nN(0)J^2S(S+1)(g-1)^2 , \quad (5.9)$$

and we estimate this parameter to be of the order of $10^{-2}(g-1)^2S(S+1)\omega_c$ from the literature.[12] For completeness we now include the Lande g value, and treat S as the total angular-momentum

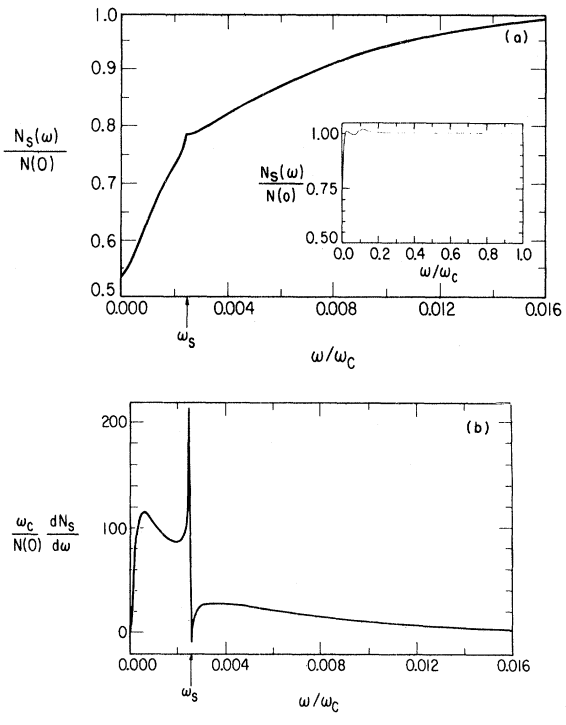

FIG. 12. (a) $N_s(\omega)$ vs ω (with spin fluctuations included) at $T=0$ for $\tau_s^{-1}=0.016\omega_c$, and $\tau_1^{-1}=0$, $\tau_2^{-1}=0.0057\omega_c$. The inset shows $N_s(\omega)$ over a wider ω scale. (b) $dN_s/d\omega$ vs ω for same parameters as in (a).

quantum number. Figure 13 corresponds to a pure superconductor at $T=T_M/3$ with $\omega_s=0.005\omega_c$ and $\tau_s^{-1}=0.032\omega_c$. While it may be noted that at $T=T_M/3$, the self-consistent Δ should be smaller than the value we chose, we have corrected for this by taking a fairly large value of τ_s. This achieves a reasonable degree of gaplessness at this temperature. Our numerical value of τ_s^{-1} was taken to be on the large side of the experimental range in order to illustrate clearly the effect of magnetic fine structure.

Figure 12(a) shows that there is sharp structure in $N_s(\omega)$ at $\omega=\omega_s$ for $T=0$. This is similar although more pronounced than found earlier (by the present authors[22]) for the case of spin-glass superconductors. That spin waves are reflected in $N_s(\omega)$ is not unexpected based on analogs[26] with phonons in strong-coupling superconductors. It should be noted from Fig. 13(a), that at higher $T\sim T_M/3$ the sharp feature in $N_s(\omega)$ is thermally smeared so that it is necessary to look at $dN_s/d\omega$ to directly observe the spin waves. Figures 12(b) and 13(b) plot this quantity for the same parameters as in Figs.

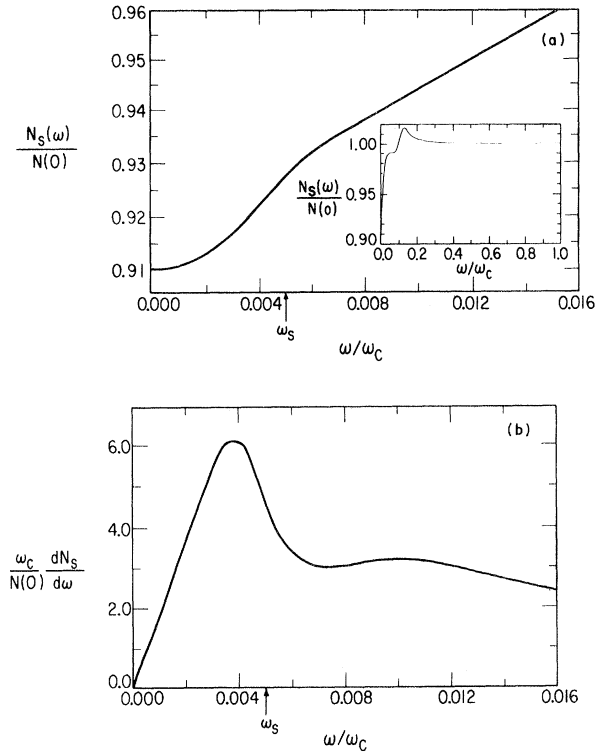

FIG. 13. (a) $N_s(\omega)$ vs ω (with spin fluctuations included) at $T=T_M/3$ for $\tau_s^{-1}=0.032\omega_c$, $\tau_1^{-1}=\tau_2^{-1}=0$. The inset shows $N_s(\omega)$ over a wider ω scale. (b) $dN_s/d\omega$ vs ω for same parameters as in (a).

12(a) and 13(a), respectively. These figures show clearly very pronounced magnetic fine structure at $\omega=\omega_s$ in $N_s(\omega)$. We have verified that the peak in $dN_s/d\omega$ at $T=T_M/3$ shifts with ω_s. It should also be noted that the additional peaks at $\omega=|(\Delta\pm H_Q)|$ are present in much the same way as they were when spin-fluctuation effects were neglected. This may be seen in the insets of Figs. 12(a) and 13(a).

VI. CONCLUSIONS

We summarize here the qualitative conclusions of the present paper. Our emphasis is on results which are experimentally verifiable. These conclusions may be divided into three categories: those pertaining to (A) nondisordered AF superconductors, (B) impurity effects, and (C) spin-fluctuation effects in AF superconductors.

In category (A) we showed that:

(i) The order parameters $\Delta_{\pm Q}$ are of negligible magnitude compared to the usual BCS order parameter. This result, obtained for 3D systems, further argues against the existence of the proposed[4,7] "new pairing state" for AF superconductors.

(ii) The superconducting density of states $N_s(\omega)$ for a 3D system with a spherical Fermi surface is strictly zero only at $\omega=0$ (for $H_Q>\Delta$). A subsidiary fine structure is found at higher frequencies $\omega=|\Delta\pm H_Q|$. Thus, even without impurities or spin fluctuations, a pure AF superconductor would be "nearly" gapless. This derives from the fact that the molecular field, H_Q, significantly alters the quasiparticle energies.

(iii) A reasonable approximation for dealing with the AF superconductors is the quasi-3D approximation. However, it appears to be better the dirtier the system. In this model $N_s(\omega)$ shows a gap at $\omega=\Delta$ and diverges at $\omega=|\Delta\pm H_Q|$. We used this approximation in all numerical work on disordered superconductors.

In category (B) we found the following:

(i) In 3D AF superconductors, non-magnetic impurities can induce gaplessness. As the impurity concentration increases still further, $N_s(\omega)$ becomes more BCS-like and a gap reopens. This derives from the fact that the impurities fill in the gaps in the normal-state band structure at the AF Brillouin-zone boundary. For $\tau_1^{-1}\gtrsim 5\omega_c$, the molecular field H_Q is effectively "screened out." These results may explain why all but very dirty AF ternary superconductors have $T_M<T_c$.

(ii) The effects of magnetic impurities are simi-

lar to those in ordinary (non-AF) superconductors. However, as nonmagnetic impurities are added to a fixed concentration of magnetic impurities the system first becomes more gapless and then less so, as in category (B), item (i).

(iii) H_c^2 has a different functional dependence on temperature depending on whether the impurities are magnetic or not. For magnetic impurities we obtain curves for H_c^2 which look similar to H_{c2} measurements.[20]

In category (C) we found the following:

(i) As in the case of spin-glass superconductors,[22] the density of states $N_s(\omega)$ has fine structure at the spin-wave frequencies ω_s, due to the transverse fluctuations. This result suggests that future tunneling experiments may be used to measure the (averaged) magnon density of states, using the approach of McMillan and Rowell[26] (who treated phonon effects in strong coupling superconductors).

(ii) At finite temperatures longitudinal fluctuations will help to further reduce the gap in $N_s(\omega)$. However, because a pure AF superconductor is on the verge of gaplessness [category (A), item (ii)] and because both magnetic and non-magnetic impurities will fill in the BCS gap [category (B), items (i) and (ii)], longitudinal fluctuations may only be important in determining the temperature dependence of $N_s(0)$. This latter quantity is expected to increase with increasing T at low T, as in the case of spin-glass superconductors.[27]

(iii) Owing to the difficulty in solving our six coupled integral equations, we have not computed $H_c^2(T)$ when fluctuations are present. Based on our other calculations, we expect the following behavior. As T decreases below T_M, H_c^2 will rapidly drop due to the "turning on" of H_Q. At lower T, H_Q saturates and the temperature dependence of the longitudinal spin fluctuations dominates that of H_c^2; H_c^2 will rapidly increase with decreasing T. Thus, we expect the behavior of H_c^2 due to spin fluctuations to look similar to that obtained when only magnetic impurities are present. As discussed in category (B), item (iii), this would yield qualitative agreement with experimental H_{c2} measurements. A calculation of the more experimentally accessible quantity H_{c2} (which includes spin fluctuations) will be presented at a later date.

ACKNOWLEDGMENTS

We gratefully acknowledge L. Coffey's help with some of the H_c^2 calculations. The work of one of the authors (M.J.N.), was supported by an IBM predoctoral fellowship. This work was supported by the National Science Foundation Grant No. DMR 80-17758, and NSF Materials Research Laboratory Grant No. 79-24007.

APPENDIX: COUPLED GAP EQUATIONS FOR $\Delta, \Delta_{\pm Q}$

In the basis

$$(C_{k\uparrow}^\dagger \;\; C_{-k\downarrow} \;\; C_{k+Q\uparrow}^\dagger \;\; C_{-k-Q\downarrow}) ,$$

the Green's function $G_0^{-1}(k,i\omega_n)$ is

$$G_0^{-1}(k,i\omega_n)=i\omega_n-\mathscr{H}^{\rm mf}=i\omega_n-\epsilon_s\sigma_3-\epsilon_a\rho_3\sigma_3+H_Q\rho_1+\Delta\sigma_1+\Delta_Q^+\rho_1\sigma_1-\Delta_Q^-\rho_2\sigma_2 , \tag{A1}$$

where

$$\epsilon_{\substack{s\\a}} =\tfrac{1}{2}(\epsilon_k \pm \epsilon_{k+Q})$$

and

$$\Delta_Q^\pm=\tfrac{1}{2}(\Delta_{-Q}\pm\Delta_Q)$$

After inverting G_0^{-1} to obtain G_0, we find

$$\Delta=VT\sum_m\int\frac{d^3k'}{(2\pi)^3}\mathrm{Tr}(G_0\sigma_1)$$

$$=VT\sum_m\int\frac{d^3k'}{(2\pi)^3}K^{-1}[\Delta(\omega_m^2+\epsilon_s^2+\epsilon_a^2-H_Q^2+\Delta^2+\Delta_Q^{-2}-\Delta_Q^{+2})+2H_Q(\epsilon_a\Delta_Q^-+i\omega_m\Delta_Q^+)] , \tag{A2}$$

$$\Delta_Q^- = -VT\sum_m \int \frac{d^3k'}{(2\pi)^3}\mathrm{Tr}(G_0\rho_2\sigma_2)$$

$$= VT\sum_m \int \frac{d^3k'}{(2\pi)^3}K^{-1}[\Delta_Q^-(\omega_m^2+\epsilon_s^2-\epsilon_a^2+H_Q^2+\Delta^2+\Delta_Q^{-2}-\Delta_Q^{+2})-2\epsilon_a(i\omega_m\Delta_Q^+-H_Q\Delta)]\ , \tag{A3}$$

$$\Delta_Q^+ = VT\sum_m \int \frac{d^3k'}{(2\pi)^3}\mathrm{Tr}(G_0\rho_1\sigma_1)$$

$$= VT\sum_m \int \frac{d^3k'}{(2\pi)^3}K^{-1}[\Delta_Q^+(\omega_m^2+\epsilon_s^2-\epsilon_a^2-H_Q^2-\Delta^2-\Delta_Q^{-2}+\Delta_Q^{+2})-2i\omega_m(\epsilon_a\Delta_Q^- -H_Q\Delta)]\ , \tag{A4}$$

where

$$K=(\omega_m^2+\epsilon_s^2+\epsilon_a^2+H_Q^2+\Delta^2+\Delta_Q^{-2}-\Delta_Q^{+2})^2-4(\epsilon_a\Delta_Q^- +i\omega_m\Delta_Q^+ -H_Q\Delta)^2-4\epsilon_s^2(H_Q^2-\Delta_Q^{+2})-4\epsilon_s^2\epsilon_a^2\ . \tag{A5}$$

We then carry out the ω_m summation and do the integrals over k' numerically to obtain the results of Sec. II.

---

*This work is based, in part, on a Ph.D dissertation of M. J. Nass.

†Deceased.

‡Present address: Exxon Research and Engineering Company, Linden, N.J. 07036.

[1]See for example, M. Ishikawa and O. Fischer, Solid State Commun. 24, 747 (1977).

[2]M. J. Nass, K. Levin, and G. S. Grest, Phys. Rev. Lett. 46, 614 (1981); in *Ternary Superconductors,* edited by G. K. Shenoy *et al.* (North-Holland, Amsterdam, 1981), p. 277.

[3]S. Maekawa and M. Tachiki, Phys. Rev. B 18, 4688 (1978).

[4]K. Machida, K. Nokora, and T. Matsubara, Phys. Rev. Lett. 44, 821 (1980); Phys. Rev. B 22, 2307 (1980).

[5]Yoshikazu Suzumura and A. D. S. Nagi, Phys. Rev. B 24, 5103 (1981).

[6]T. V. Ramakrishnan and C. M. Varma, Phys. Rev. B 24, 137 (1981).

[7]G. Zwicknagl and P. Fulde, Z. Phys. (in press).

[8]See, for example, K. Maki in *Superconductivity of Metals and Alloys,* edited by R. D. Parks (Dekker, New York, 1969).

[9]A. A. Abrikosov and L. P. Gorkov, Zh. Eksp. Teor. Fiz. 39, 1781 (1961) [Sov. Phys.—JETP 12, 1243 (1961)].

[10]S. Skalski, O. Betbeber-Matibet, and P. R. Weiss, Phys. Rev. 136, A1500 (1964).

[11]As pointed out in Ref. 3, in the ternary compounds there are basically two types of conduction electrons; those which mediate the RKKY interaction which orders the rare-earth spins and the superconducting electrons. Throughout this paper we will ignore the former.

[12]M. Ishikawa and J. Muller, Solid State Commun. 27, 761 (1978); R. Odermatt, M. Hardiman, and J. Van Meijel, *ibid.* 32, 1227 (1979).

[13]A. J. Freeman (private communication).

[14]The fact that we are using a spherical Fermi surface and we expect about 10% of the Fermi surface to be in region I (so that $Q\cong 0.1k_F$), necessitates taking a somewhat smaller value of Q than would be expected. However, since Q appears primarily in a weighting factor, which measures the size of region I, we don't believe our underestimate of Q is significant.

[15]In paper L1, using a four-dimensional representation, we called the pseudogap parameter $\tilde{\Delta}_Q^+$. However, in the expanded eight dimensional basis, $\tilde{\Omega}$ does not have the same symmetry as $\tilde{\Delta}_Q^+$ of paper L1 and we have, therefore, adopted a new symbol.

[16]G. Bilbro and W. L. McMillan Phys. Rev. B 14, 1887 (1976).

[17]A useful fact which follows from the constraint that both terms in $N_s(\omega)$ are positive is that the signs of $\mathrm{Im}u^{\pm}$ and $\mathrm{Re}[1-(u^{\pm})^2]^{1/2}$ are related at $\omega=0$. [We consider this case, since at $\omega=0$ either $u^{\pm}$ is zero or pure imaginary, owing to the symmetry $u(\omega)=-u^*(-\omega)$.]

[18]In the quasi-3D limit we are forced to take a somewhat smaller H_Q than would be expected experimentally and than we considered in paper L1. This derives from the fact that in the quasi-3D approximation, the system is driven normal for moderately large H_Q. This could be compensated for by reducing γ below 1 or 2%. However, we chose to reduce H_Q, instead.

[19]We expect our density-of-states calculation to be accurate to within 1%. However, derived quantities

such as H_c^2 are probably only accurate to within 15%.

[20]M. Ishikawa, O. Fisher, and J. Muller, J. Phys. (Paris) Colloq. 6, 1379 (1978).

[21]M. J. Nass, K. Levin, and G. S. Grest, Phys. Rev. B 23, 1111 (1981). This paper omitted an overall minus sign on the right-hand side of Eq. (2.9).

[22]M. J. Nass, K. Levin, and G. S. Grest, Phys. Rev. Lett. 45, 2070 (1981).

[23]In principle, since we fixed the direction of $\langle \vec{S}_Q \rangle$ in our molecular-field calculations, the susceptibility $\chi(q,\omega)$ should not be taken as isotropic. However, as noted in the text, unless one makes the isotropy assumption, the self-energy, gap, etc., are functions of $\vec{k}$. To avoid this extreme complication we are forced to take a spherical average of χ.

[24]While a sum rule of the correlation function $S(q,\omega) \equiv B(q,\omega)/(1-e^{-\beta\omega})$ provided an important constraint in our ealier work on spin glasses (see Ref. 21), it is of less relevance to the present case because (a) the $\phi(q)$ term is presumed to be more important, due to the complexity of the Fermi surface, and (b) the correlation function explicitly contains a temperature-dependent term $\langle \vec{S}_i \rangle \cdot \langle \vec{S}_j \rangle$ subtracted from $\langle \vec{S}_i(t) \cdot \vec{S}_j(0) \rangle$. In the spin-glass case this subtracted term (when properly configuration averaged) is zero.

[25]G. S. Grest, K. Levin, and M. J. Nass, Phys. Rev. B 21, 1219 (1980).

[26]W. L. McMillan and J. M. Rowell, in *Superconductivity,* edited by R. D. Parks (Dekker, New York, 1969).

[27]I. Schuller, R. Orbach, and P. M. Chaikin, Phys. Rev. Lett. 41, 1413 (1978).